Talk at MIT 2003

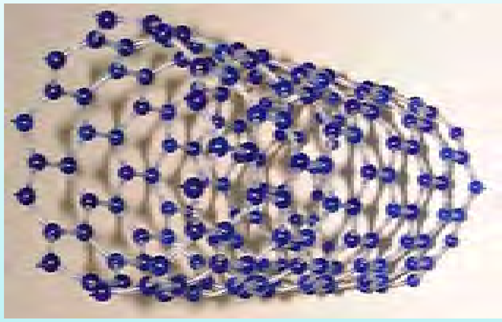

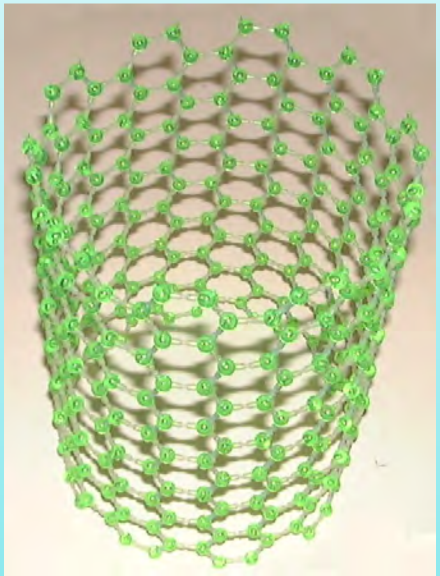

Topological Order in Superconductivity and Carbon Nano-Structures

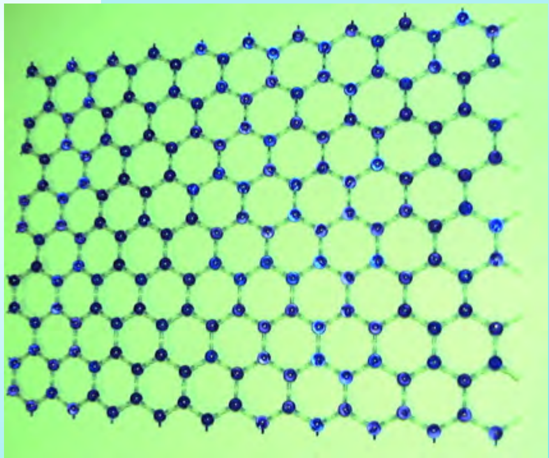

Y. Hatsugai

Dept. of Applied Physics, Univ. of Tokyo

with S. Ryu, M. Kohmoto

Plan of talk today

- (Part of) Target Phenomena
- Topological Aspect of QHE
- Topological Aspect of Superconductors
  - Dirac Monopoles and Topological Numbers (Simple case)
  - Generic Consideration: Non-Abelian Gauge Structures
  - Zero Bias Conductance Peak and local Time Reversal Symmetry Breaking

(Peierls Instability of edge states)

- Topological Aspects of Carbon Nano-Structures
  - Topological Consideration of Zero Modes Edge states
  - Localized Spin moments: generalized Kondo Problem
  - Localized Spin Moments as a Local Chiral Symmetry Breaking

(Peierls Instability of edge states)

Zero Bias Conductance Peak
in Anisotropic Superconductivity

VOLUME 83, NUMBER 22 PHYSICAL REV

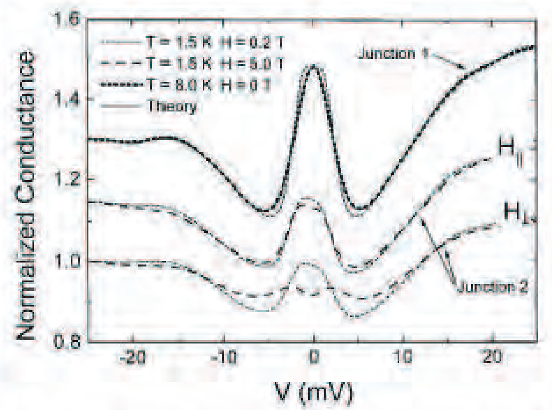

FIG. 1. The temperature dependence of the in-plane tunneling conductance of (110)-YBCO/Pb junctions as function of bias and magnetic field is shown. The field H is always applied parallel to the junction interface, and either parallel or perpendicular to the YBCO ab planes, as labeled. The theoretical curve (solid line) is calculated using the FRS theory [11], as described in the text. For junction 2, low-temperature spectra for low and high applied magnetic field are shown. Note the field-induced splitting in the ZBCP is strongly anisotropic with respect to the field orientation. Data obtained on junction 1 show reproducibility between junctions for data taken at low temperature and field ($T = 1.5$ K, $H = 0.2$ T). Zero-field data taken at a temperature above the T_c of Pb is also shown for junction 1.

Zero Energy Boundary States of Anisotropic Superconductivity

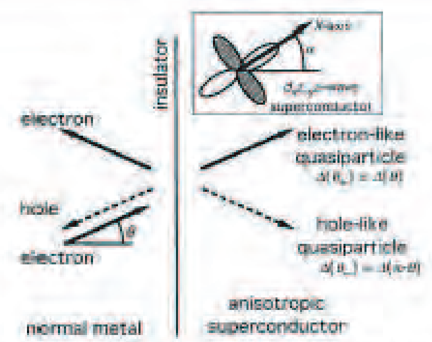

FIG. 1. Schematic illustration of the reflection and transmission processes at the interface. In this figure the quantities θ and α express the injection angle of the electron and the angle between the normal vector of the interface and the x axis of the $d_{x^2-y^2}$-wave superconductor, respectively.

Tanaka-Kashiwaya

L. J. Buchholtz,G. Zwicknagl, Phys. Rev. B 23, 5788 (1981) (p wave)

C.-R. Hu, Phys. Rev. Lett. 72, 1526 (1994) (d wave)

S. Kashiwaya, Y. Tanaka, Phys. Rev. Lett. 72, 1526 (1994)

M. Matsumoto and H. Shiba, JPSJ, 1703 (1995)

(fig.) M. Aprili, E. Badica, and L. H. Greene,Phys. Rev. Lett. 83, 4630 (1999)

Localized Boundary State in Carbon Sheet (1)

Tight-binding Model Calculation

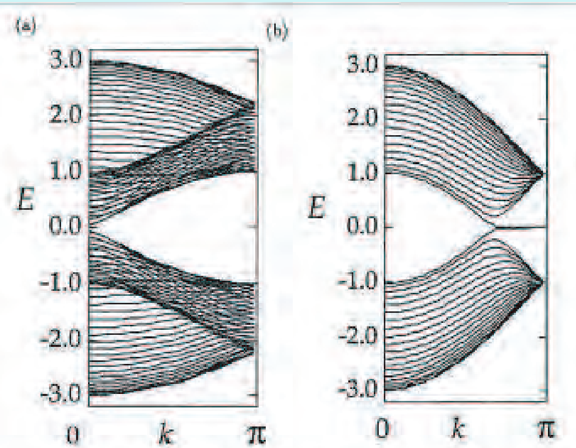

Fig. 2. Band structure of (a) armchair and (b) zigzag ribbons with width $N = 20$.

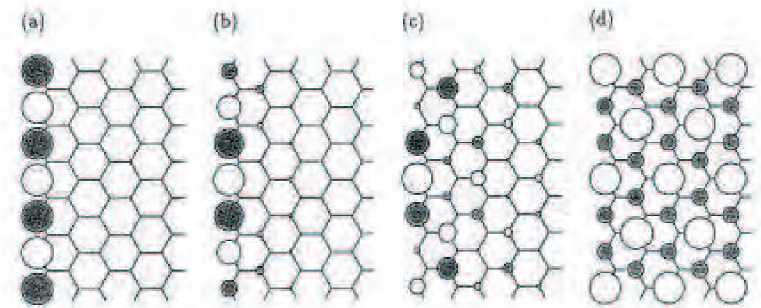

Fig. 3. Schematic figures of the real part of analytic solutions for the edge state in semi-infinite graphite, when (a) $k = \pi$, (b) $8\pi/9$, (c) $7\pi/9$ and (d) $2\pi/3$.

" Peculiar Localized State at Zigzag Graphite Edge " M. Fujita, K. Wakabayashi, K. Nakada and K. Kusakabe, JPSJ 65, 1920 (1996)

Localized Boundary State in Carbon Sheet (2)

Local Spin Density Functional Appr. Calculation

VOLUME 87, NUMBER 14 PHYSICAL REVIEW LETTERS 1 OCTOBER 2001

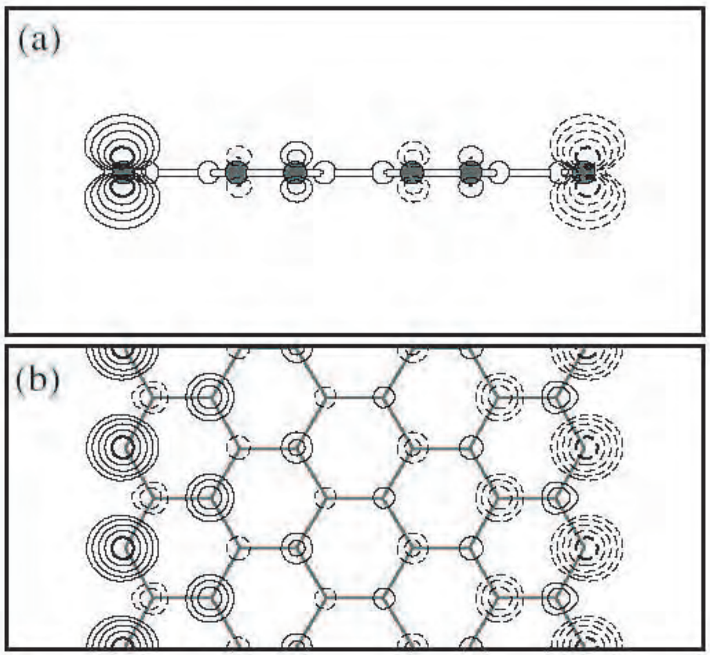

FIG. 1. Contour plots of spin density $n_\uparrow(\boldsymbol{r}) - n_\downarrow(\boldsymbol{r})$ (a) on a plane perpendicular to a graphite flake with zigzag edges and (b) on a plane including the graphite flake. In (a) the edges are perpendicular to the plane and C atoms on the plane are depicted by shaded circles. Positive and negative values of the spin density are shown by solid and dashed lines, respectively. Each contour represents twice (or half) the density of the adjacent contour lines.

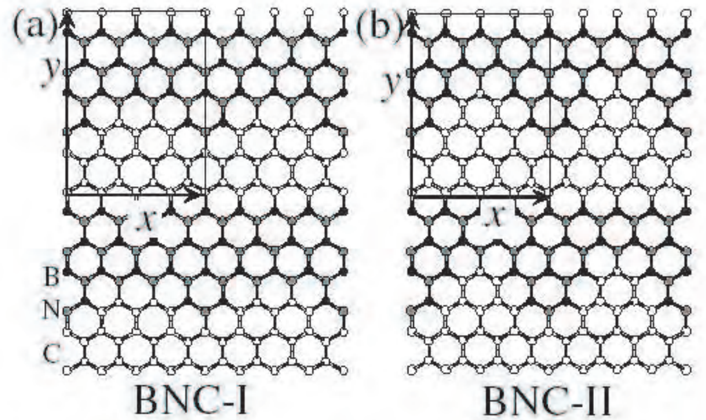

FIG. 2. Top views of fully optimized BNC heterosheets. (a) BNC-I and (b) BNC-II. White, shaded, and black circles denote C, B, and N atoms, respectively. The rectangle in each figure denotes the unit cell.

B, N, and C atoms have been observed indeed [8–10]. Second, the phase separation of graphite and BN regions leading to the striped structures above is energetically favorable. In fact, we have performed the total-energy calculations for graphite, BN, BC, and NC heterosheets by DFT. The calculated bond energies of B-C and N-C are smaller than that of graphite by 1.52 and 0.81 eV, respectively. On the other hand, the bond energy of B-N is smaller than that of graphite only by 0.31 eV. Third, undulation

"Magnetic Ordering in Hexagonally Bonded Sheets with First-Row Elements",
Okada, Oshiyama, Phys. Rev. Lett. 87, 146803 (2001)

Appearance of Topological Order in Condensed Matter (X.G.Wen)

- Quantum Hall Effects (Integer & Fractional)
  - Energy Gap and Quatization of Hall Conductance
  - Topological Characterization of Hall Conductance
  - Bulk $\leftrightarrow$ Edge
  - Integer $\leftrightarrow$ Fractional : Composite Fermion Picture
- Spin Chain with Integral Spin
  - Energy Gap with Topological Origin
  - Kennedy Triplet with finite Length Spin Chains (Edge States)
- Polyacetylene :(SSH Model)
- High-T_C, Chiral Spin State, Anyon-Superconductivity, Fractionalization
- Chirality Order in Itinerant Magnetism
- Polarization of Insulators, KSV formula
- Anisotropic Superconductivity $\&$ Superfluidity
  - Dirac Monopoles and Topological Origin of Zero Bias Peaks
- Carbon Nano-Structures
  - Various Shape of Edges and Localized Zero Modes

Hofstadter's Butterfly and the Topological Integers

Energy spectrum of the square lattice (2D) with magnetic fi eld ϕ per plaquette

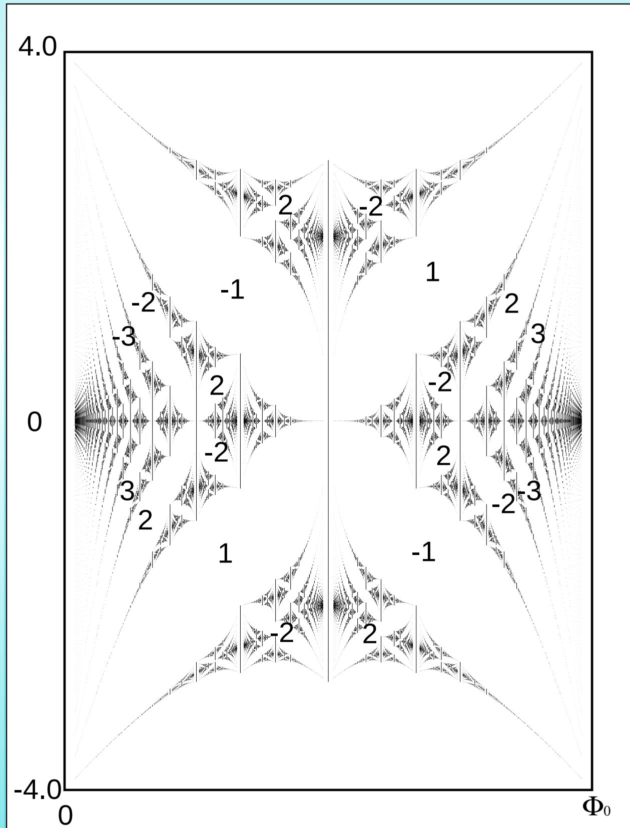

$$H = \sum_{\langle ij\rangle} c_i^\dagger e^{i\theta_{ij}} c_j + h.c.$$

$$\circlearrowleft\!\!\sum_{j\in\langle ij\rangle} \theta_{ij} = 2\pi\phi_i = 2\pi\phi$$

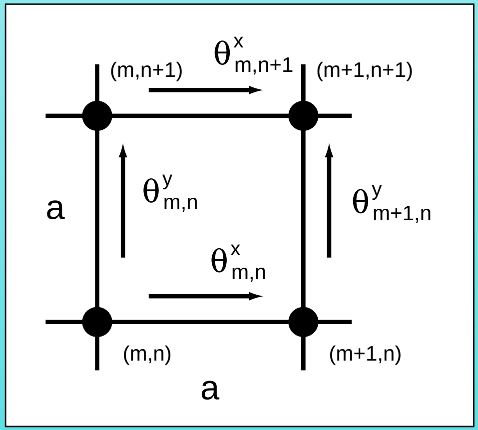

- Diagram is self similar :Fractal
- Integer = Topological integer = Laughlin's unkown n

  : Hall conductance in unit $\frac{e^2}{h}$ when the Fermi energy is at the gap.

Topological Aspect of the Quantum Hall Effect

Bulk $\leftrightarrow$ Edge states (Explicite observable)

(Almost always) with topological ordered states

Laughlin's unkown interger n has several topological expressions.

- σ_{xy} as a topological Invariant by bulk states
  - Chern number, C , TKNN'82, PRL 49, 405
    - Total vorticity of the relative phase of the Bloch function on the Brillouin zone.
- σ_{xy} as a topological Invariant by edge states
  - Intersection number, I, Y.H.'93, PRB48, 11853, PRL 71, 3697
    - Intersectin number of the zero of the Bloch function (Edge States) on the complex energy surface with a closed loop (an energy band).
- The above 2 Different Topological Integers are Equal.

$$\boxed{C = I}$$

- Bulk and Edge descriptions are equivalent.

TKNN Formula (Chern number)
(TKNN'82, PRL 49, 405)

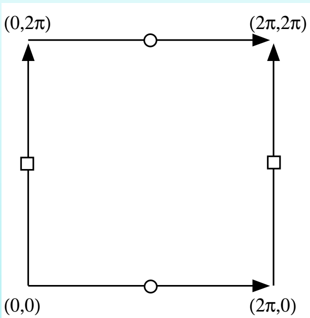

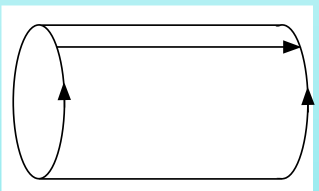

$$\begin{aligned}
\sigma_{xy}^{j,\,\mathrm{bulk}} &= -\frac{e^2}{h}C, \quad C = \sum_{\ell=0}^{j} c_\ell \\
c_\ell &= \frac{1}{2\pi i}\int_{T_{MBZ}} d\vec{S}_k \cdot \vec{\mathcal{B}}^\ell \\
\vec{\mathcal{B}}^\ell &= \mathrm{rot}_k\, \vec{\mathcal{A}}^\ell \\
\vec{\mathcal{A}}^\ell &= \langle \psi^\ell | \vec{\nabla}_k \psi^\ell \rangle
\end{aligned}$$

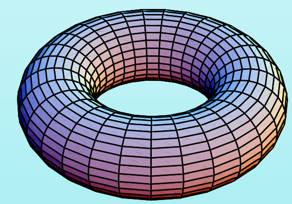

$|\psi^\ell(\vec{k})\rangle = \begin{pmatrix} \Psi_1 \\ \vdots \\ \Psi_q \end{pmatrix}$:Bloch function of the loweset ℓ-th band. ($\sum_{k=1}^{q} |\Psi_k|^2 = 1$).

- ♦ T_{MBZ}: (Magnetic) Brilluine zone: topologically Torus
- ♦ $\rightarrow$ No boundary $\rightarrow C = 0$ by the Stokes Theorem ?
- ♦ No! Look for singularities!

Chern number and Vortex (Kohmoto ’85, Hatsugai ’93)

$$H(k)|\psi^\ell(\vec{k})\rangle = \epsilon^\ell(\vec{k})|\psi^\ell(\vec{k})\rangle, \ \ \langle\psi^\ell(\vec{k})|\psi^\ell(\vec{k})\rangle = 1$$

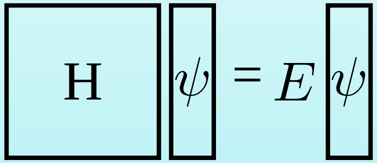

- Phase of $|\psi^\ell(\vec{k})\rangle$ is arbitrary for each k
- $\rightarrow$ Gauge Freedom for $\mathcal{A} = \langle\psi|\vec{\nabla}_k\psi\rangle$

$$|\psi^\ell(\vec{k})\rangle^A = e^{i\xi_{AB}}|\psi^\ell(\vec{k})\rangle^B \qquad \vec{\mathcal{B}}^{\ell,A} = \vec{\mathcal{B}}^{\ell,B}$$

$$\vec{\mathcal{A}}^{\ell,A} = i\vec{\nabla}\xi_{AB} + \vec{\mathcal{A}}^{\ell,B} \qquad c_\ell^A = c_\ell^B$$

The Chern number is invariant

Patch work of the BZ

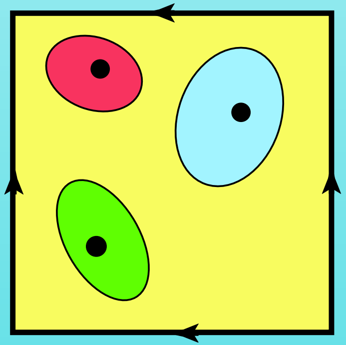

- Gauge fi xing to calculate C
  - Take, say, ψ_q to be real positive! It fails when $\psi_q = 0$!!
  - Need to take different gauge then, say, ψ_1 to be real positive!
- Patch work of the T_{MBZ} to calculate C

$$T_{MBZ} = Z \cup NZ$$

$$Z = \cup_m R_m, \quad NZ = T_{MBZ} \setminus Z$$

where R_ℓ include a zero of $\psi_q(k)$.

Chern number and Vortex (Cont.)

$$|\psi\rangle^Z = |\psi\rangle e^{-i\mathrm{Im}\ \log|\psi\rangle_1}, \quad \mathcal{A}^Z = {}^Z\langle\psi|\nabla\psi\rangle^Z = \langle\psi|\nabla\psi\rangle - i\nabla\mathrm{Im}\ \log|\psi\rangle_1 \quad \psi \in Z$$

$$|\psi\rangle^{NZ} = |\psi\rangle e^{-i\mathrm{Im}\ \log|\psi\rangle_q}, \quad \mathcal{A}^{NZ} = {}^{NZ}\langle\psi|\nabla\psi\rangle^{NZ} = \langle\psi|\nabla\psi\rangle - i\nabla\mathrm{Im}\ \log|\psi\rangle_q \quad \psi \in NZ.$$

This is well-defined since $|\psi\rangle_1$ is non zero in Z and $|\psi\rangle_q$ is non zero in NZ.

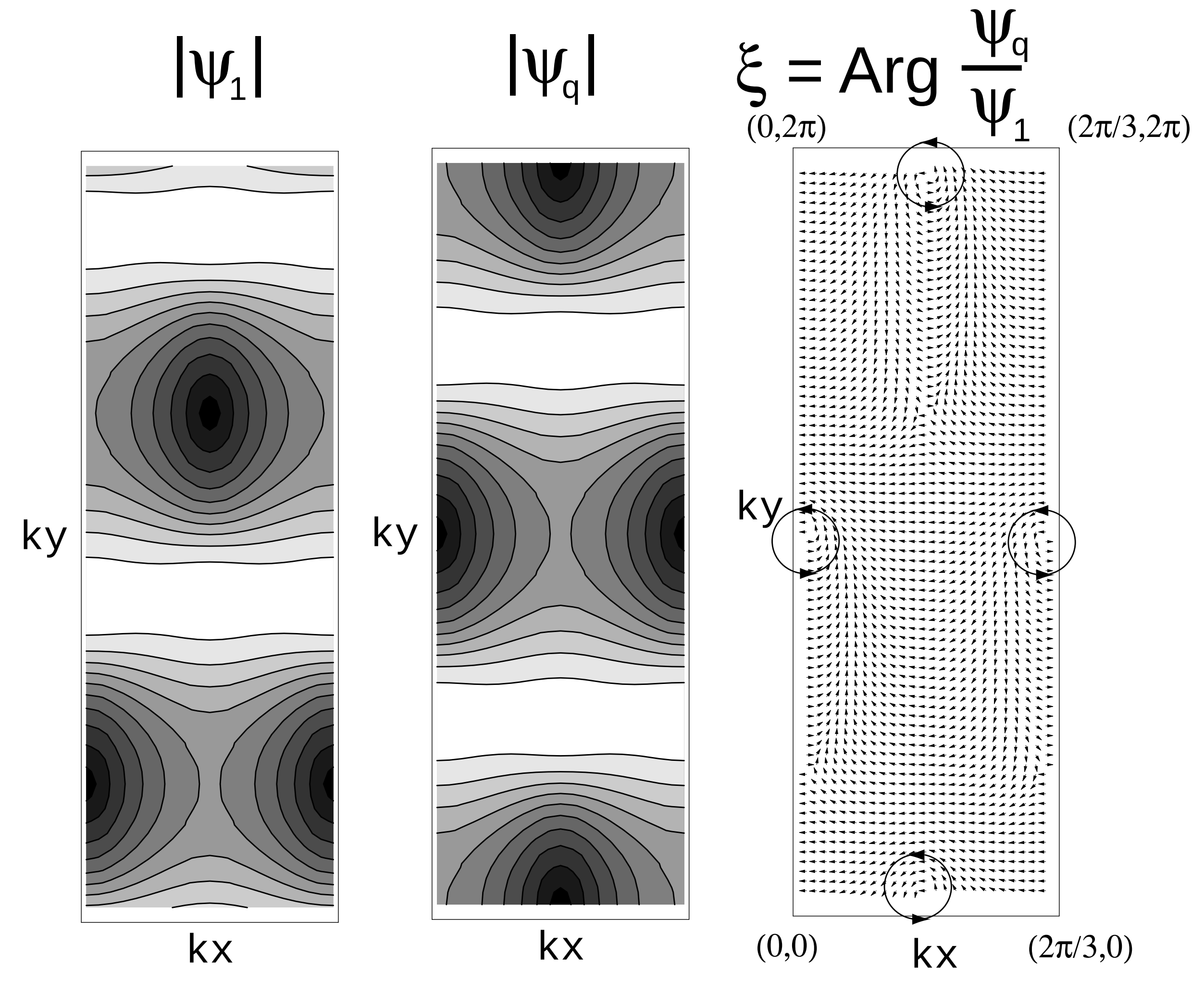

Applying the Stokes theorem in each region,

$$\begin{aligned} c_\ell &= \frac{1}{2\pi i}\int_Z d\boldsymbol{S}_k \cdot \mathrm{rot}_k\, \vec{\mathcal{A}}^Z \\ &\quad + \frac{1}{2\pi i}\int_{NZ} d\boldsymbol{S}_k \cdot \mathrm{rot}_k\, \vec{\mathcal{A}}^{NZ} \\ &= \frac{1}{2\pi i}\oint_{\partial Z} d\boldsymbol{r} \cdot (\vec{\mathcal{A}}^Z - \vec{\mathcal{A}}^{NZ}) \\ &= -\sum_m \frac{1}{2\pi}\oint_{\partial R_m} d\boldsymbol{r} \cdot \vec{v}(\vec{k}) \end{aligned}$$

$$v(\vec{k}) = \vec{\nabla}\mathrm{Im}\ \log\frac{|\psi\rangle_1}{|\psi\rangle_q}$$

The Chern number c_ℓ is given by the total vorticity.

Chern nu t.)

$$|\psi\rangle^Z = \ |\psi\rangle e^{-i\mathrm{I}} \quad \langle\psi|\nabla\psi\rangle - i\nabla \mathrm{Im}\ \log|\psi\rangle_1 \quad \psi\in Z$$

$$|\psi\rangle^{NZ} = |\psi\rangle e^{-i\mathrm{Im}} \quad \langle\psi|\nabla\psi\rangle - i\nabla \mathrm{Im}\ \log|\psi\rangle_q \quad \psi\in NZ.$$

This is well-defined is non zero in NZ.

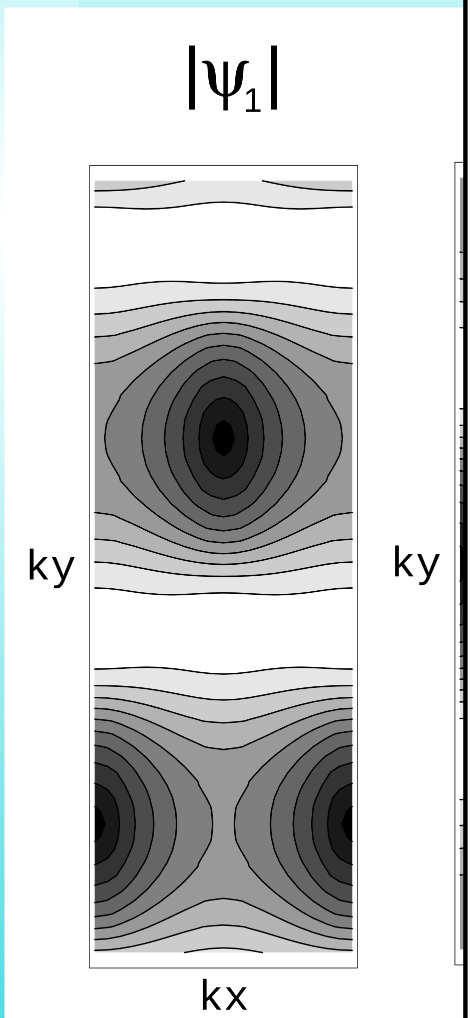

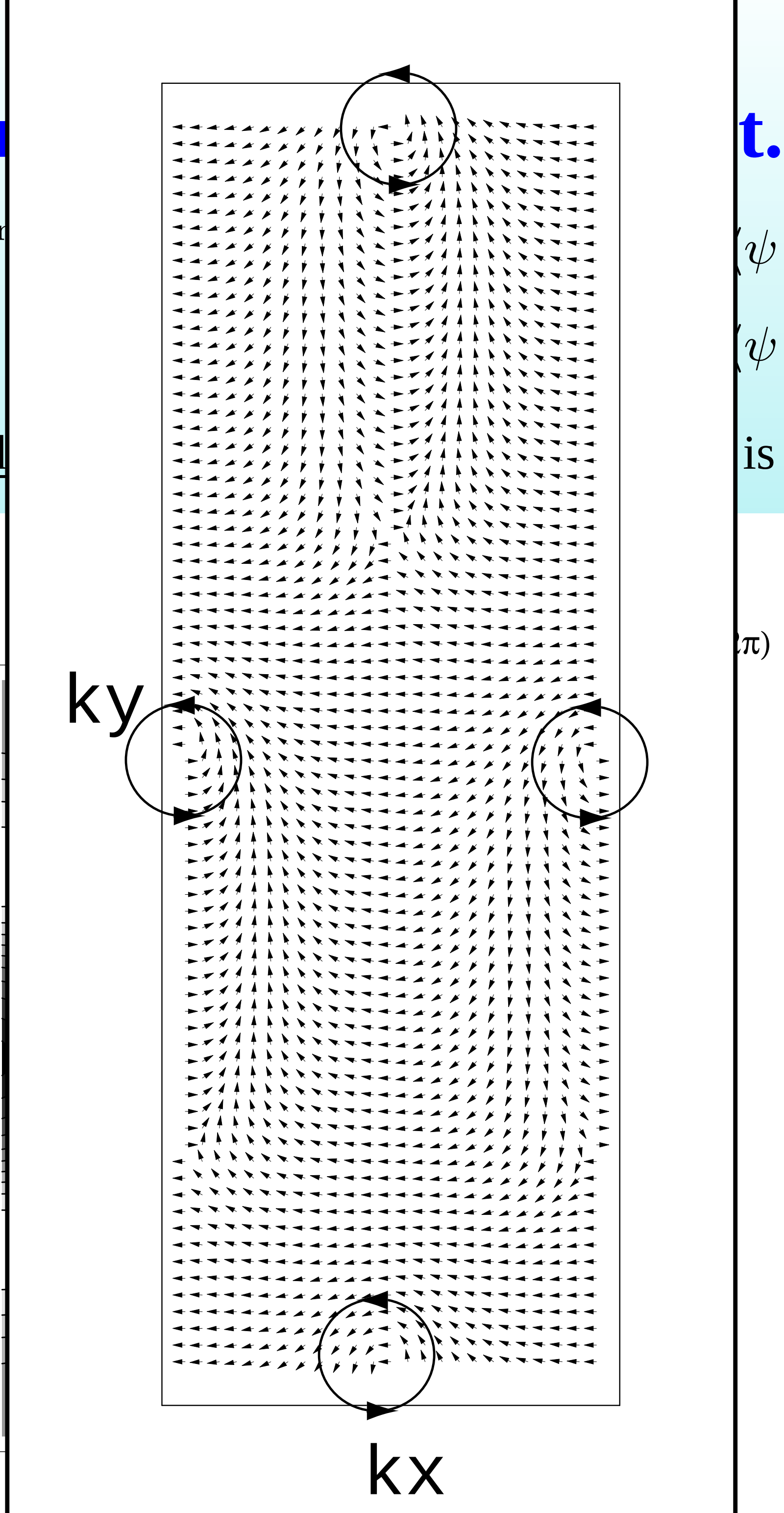

Applying the Stokes theorem in each region,

$$c_\ell = \frac{1}{2\pi i}\int_Z d\boldsymbol{S}_k \cdot \mathrm{rot}_k\,\vec{\mathcal{A}}^Z + \frac{1}{2\pi i}\int_{NZ} d\boldsymbol{S}_k \cdot \mathrm{rot}_k\,\vec{\mathcal{A}}^{NZ}$$

$$= \frac{1}{2\pi i}\oint_{\partial Z} d\boldsymbol{r}\cdot(\vec{\mathcal{A}}^Z - \vec{\mathcal{A}}^{NZ})$$

$$= -\sum_m \frac{1}{2\pi}\oint_{\partial R_m} d\boldsymbol{r}\cdot\vec{v}(\vec{k})$$

$$v(\vec{k}) = \vec{\nabla}\mathrm{Im}\ \log\frac{|\psi\rangle_1}{|\psi\rangle_q}$$

The Chern number c_ℓ is given by the total vorticity.

Apply it to the Superconductivity

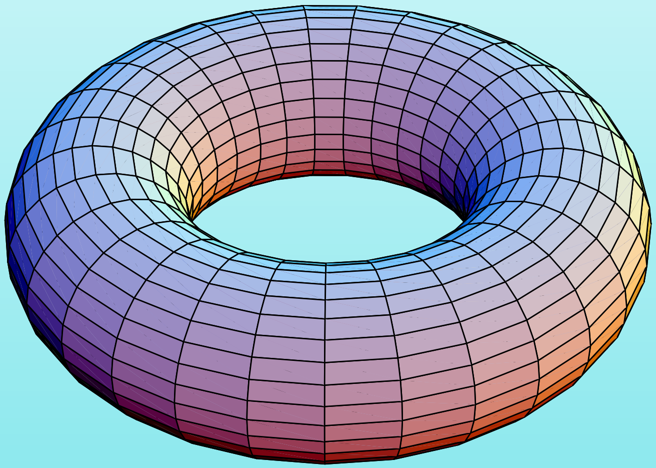

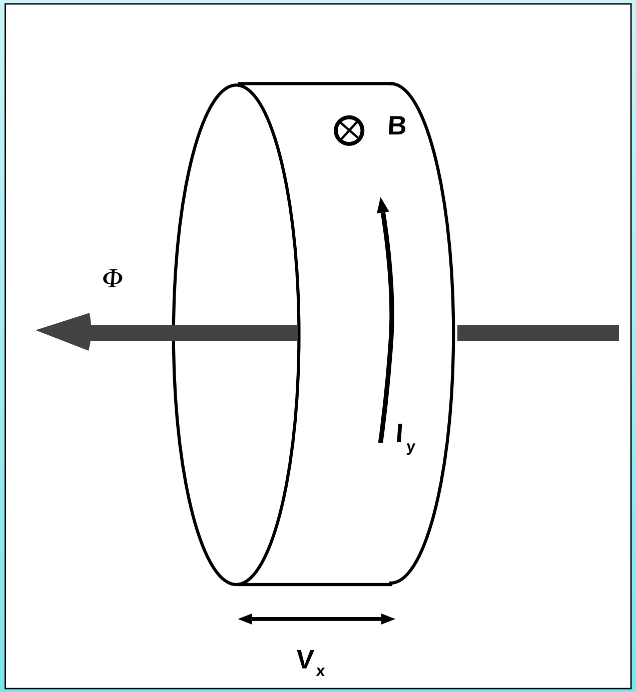

Bogoliuvov-de Gennes Hamiltonian (simple case)

$$H[\{c_i, c_i^\dagger\}] = \sum_{ij} t_{ij}^\sigma c_{i\sigma}^\dagger c_{j\sigma} - \mu \sum_{i\sigma} c_{i\sigma}^\dagger c_{i\sigma} + \sum_{ij} \left(\Delta_{ij} c_{i\uparrow}^\dagger c_{j\downarrow}^\dagger + \Delta_{ij}^* c_{j\downarrow} c_{i\uparrow} \right)$$

$$= \boxed{\sum_{ij} \boldsymbol{c}_i^\dagger \boldsymbol{h}_{ij} \boldsymbol{c}_j} + const. \qquad \boldsymbol{c}_i = \begin{pmatrix} c_{i\uparrow} \\ c_{i\downarrow}^\dagger \end{pmatrix}, \quad \boldsymbol{h}_{ij} = \begin{pmatrix} \tilde{t}_{ij}^\uparrow & \Delta_{ij} \\ \Delta_{ji}^* & -\tilde{t}_{ji}^\downarrow \end{pmatrix}$$

- Bilinear in Fermion operators $\{d_i^\sigma\}$ after the unitary transfomation

$$\begin{cases} d_i^\uparrow = c_i^\uparrow \\ d_i^\downarrow = c_i^{\dagger\downarrow} \end{cases}, \quad H[\{d_i, d_i^\dagger\}] = H[\{c_i, c_i^\dagger\}]$$

- Analogue of the QHE with flux $\phi = \frac{1}{2}$
- Topological Argument is applied
- Hall conductance σ_{xy} in $\{d_i^\sigma\}$

  $\leftrightarrow$ Spin Hall conductance $\sigma^{\text{spin}}{}_{xy}$ in $\{c_i^\sigma\}$

Possible Order Parameters

$$H^{BdG} = \sum_{ij} t^{\sigma}_{ij} c^{\dagger}_{i\sigma} c_{j\sigma} - \mu \sum_{i\sigma} c^{\dagger}_{i\sigma} c_{i\sigma} + \sum_{ij} \left(\Delta_{ij} c^{\dagger}_{i\uparrow} c^{\dagger}_{j\downarrow} + \Delta^{*}_{ij} c_{j\downarrow} c_{i\uparrow} \right)$$

$$\sum_{ij} (\Delta_{ij} c^{\dagger}_{i\uparrow} c^{\dagger}_{j\downarrow} + \Delta^{*}_{ij} c_{j\downarrow} c_{i\uparrow})$$

$$= \sum_{i \preceq j} \Delta_{ij} \begin{array}{lll} (c^{\dagger}_{i\uparrow} c^{\dagger}_{j\downarrow} + c^{\dagger}_{i\downarrow} c^{\dagger}_{j\uparrow}) + h.c. & \text{Parity Even: (Singlet)} & \Delta_{ij} = \Delta_{ji} \\ (c^{\dagger}_{i\uparrow} c^{\dagger}_{j\downarrow} - c^{\dagger}_{i\downarrow} c^{\dagger}_{j\uparrow}) + h.c. & \text{Parity Odd: (Triplet)} & \Delta_{ij} = -\Delta_{ji} \end{array}$$

Singlet:

s-wave

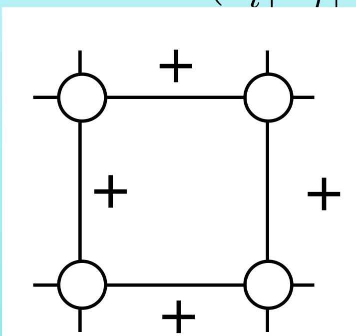

$d_{x^2-y^2}$

high-T_C

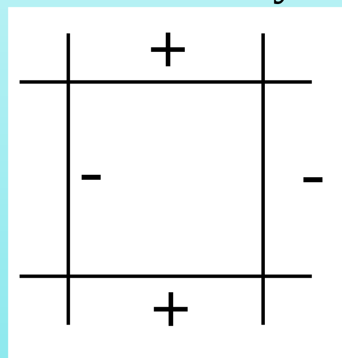

$d_{x^2-y^2} + id_{xy}$

Laughlin

T-breaking

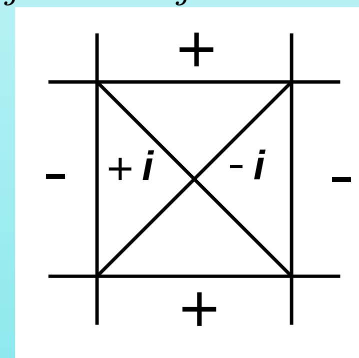

Quasiparticle dispersion

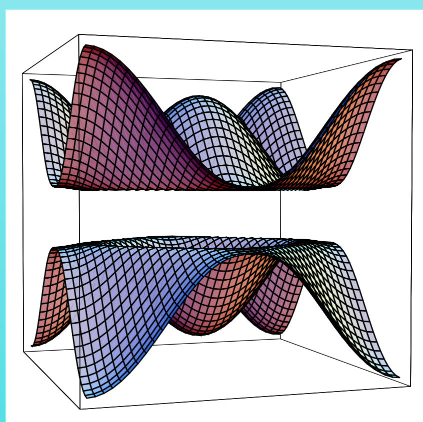

Uniform gap on the Fermi line

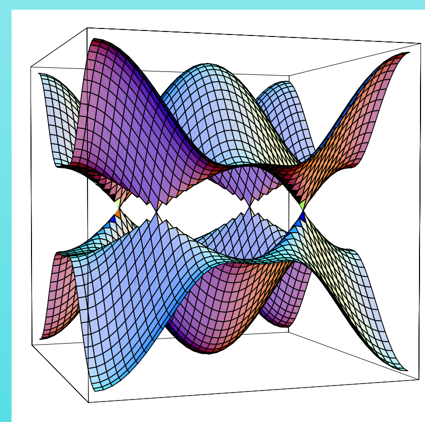

4 Dirac Nodes

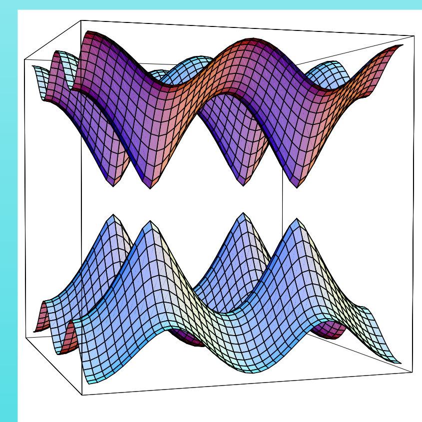

Gap openning

Possible Order Parameters – cont.—

Triplet:

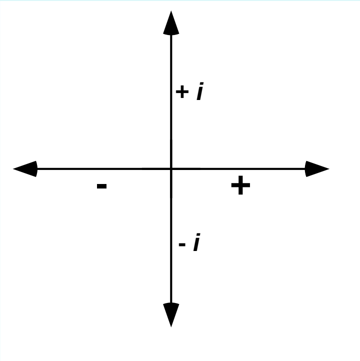

Chiral p wave
with chemical potential μ

$\mu = 0$

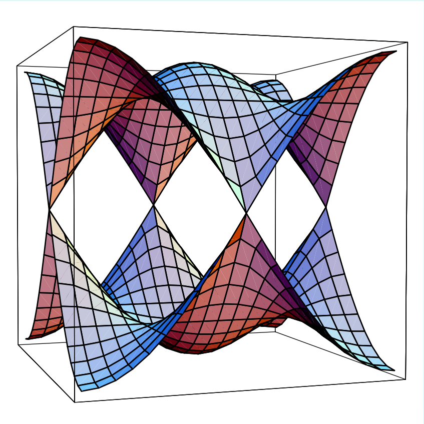

1 Dirac Node at zone boundary

$\mu = -0.5$

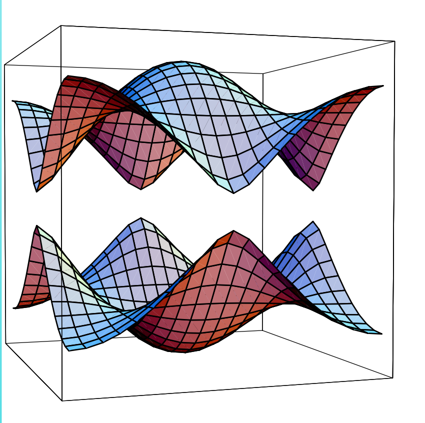

Gap Openning

$\mu = -4$

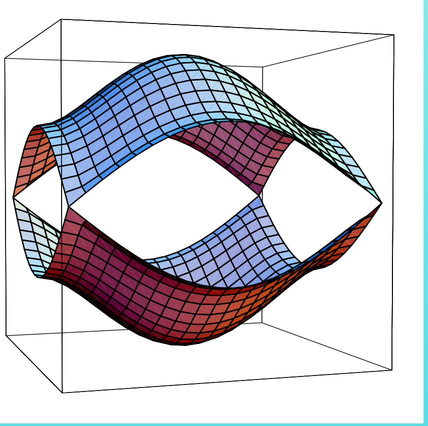

One Dirac Node at zone corner

$\mu = -5$

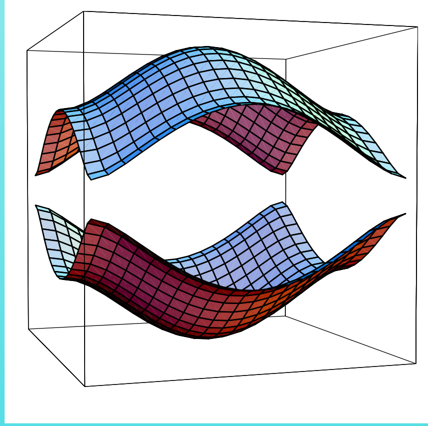

Gap Openning Again

Chern Number in the Superconductivity

$$H^{BdG} = \sum_k \boldsymbol{c}^\dagger(\boldsymbol{k})\boldsymbol{h}(\boldsymbol{k})\boldsymbol{c}(\boldsymbol{k}), \qquad \boldsymbol{c}^\dagger(\boldsymbol{k}) = (c_\uparrow^\dagger(\boldsymbol{k}), c_\downarrow(\boldsymbol{k}))$$

$$\boldsymbol{h}(\boldsymbol{k}) = \begin{pmatrix} \epsilon^\uparrow(\boldsymbol{k}) & \Delta(\boldsymbol{k}) \\ \Delta^*(\boldsymbol{k}) & -\epsilon^\downarrow(-\boldsymbol{k}) \end{pmatrix}, \qquad \begin{array}{l} \epsilon^\sigma(\boldsymbol{k}) = \sum_j e^{-i\boldsymbol{k}\cdot\boldsymbol{r}_j} t^\sigma(j) \\ \Delta(\boldsymbol{k}) = \sum_j e^{-i\boldsymbol{k}\cdot\boldsymbol{r}_j} \Delta(j) \end{array}$$

The Chern number C for the negative energy state $|\boldsymbol{k}\rangle$, $\boldsymbol{h}(\boldsymbol{k})|\boldsymbol{k}\rangle = -E(\boldsymbol{k})|\boldsymbol{k}\rangle$,

$$C = \frac{1}{2\pi i}\int_{T^2} d\boldsymbol{S}_k \cdot \boldsymbol{B}_k$$

$$\boldsymbol{B}_k = \mathrm{rot}_k\, \boldsymbol{A}_k$$

$$\boldsymbol{A}_k = \langle \boldsymbol{k}|\boldsymbol{\nabla}_k|\boldsymbol{k}\rangle$$

- The spin Hall conductance $\sigma_{xy}^{spin} = -\frac{e^2}{h}C$
- C is a topological integer $\longrightarrow$ stable against small perturbation

To change C, the energy gap has to collapse

- $\longrightarrow$ Use it to characterize the superconducting state!
  Characterization by the topological order

Chern Number and the Winding Number

$$\boxed{\begin{aligned} C &= -N_{\text{winding}} \\ N_{\text{winding}} &= \sum_{\ell} \frac{1}{2\pi} \oint_{\partial R_\ell} d\boldsymbol{k} \cdot \boldsymbol{\nabla}_k \mathrm{Im}\ \log \frac{|\boldsymbol{k}\rangle_1}{|\boldsymbol{k}\rangle_2} \end{aligned}}$$

The summation is over the poles of $\frac{|\boldsymbol{k}\rangle_1}{|\boldsymbol{k}\rangle_2}$ (R_ℓ is a small area around each pole)

Example:

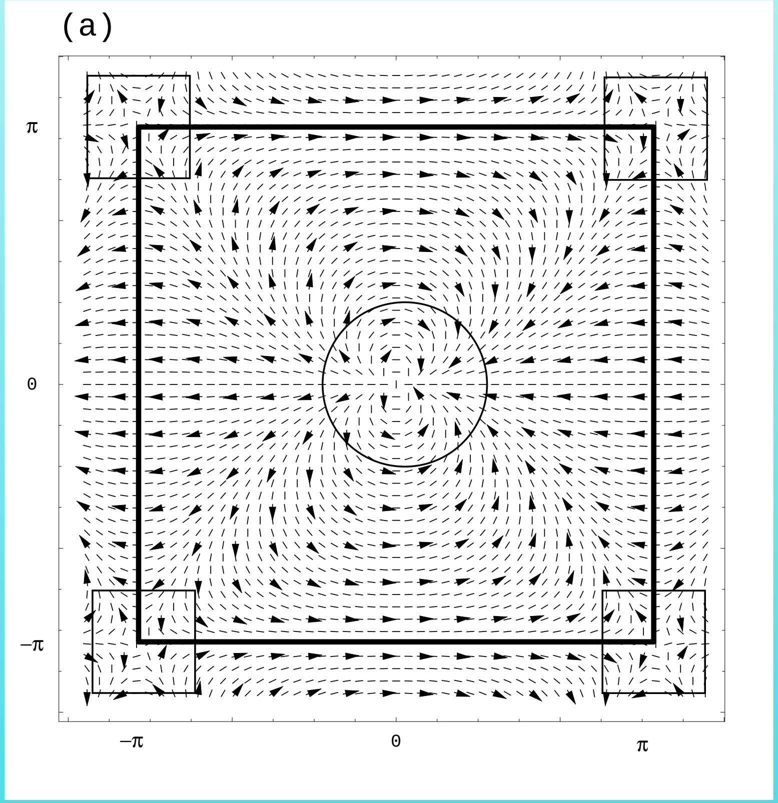

$d_{x^2-y^2} + id_{xy}$

$$\boxed{C = 2\mathrm{sgn}\ \frac{\Delta_{x^2-y^2}}{\Delta_{xy}}}$$

Sentil-Marston-Fisher

Morita-Hatsugai

Read-Green

Berry's parametrization in the Superconductivity

Y. Hatsugai and S. Ryu, PRB 65, 212510 (2002)

$$\boldsymbol{h}(\boldsymbol{k}) = \begin{pmatrix} \epsilon(\boldsymbol{k}) & \Delta(\boldsymbol{k}) \\ \Delta^*(\boldsymbol{k}) & -\epsilon(\boldsymbol{k}) \end{pmatrix} \boxed{= \boldsymbol{R}(\boldsymbol{k}) \cdot \boldsymbol{\sigma}}$$

$$\boldsymbol{R}(\boldsymbol{k}) = (R_x(\boldsymbol{k}), R_y(\boldsymbol{k}), R_z(\boldsymbol{k})) = (\mathrm{Re}\,\Delta(\boldsymbol{k}), -\mathrm{Im}\,\Delta(\boldsymbol{k}), \epsilon(\boldsymbol{k}))$$

$$\boldsymbol{\sigma} = (\sigma_x, \sigma_y, \sigma_z)$$: Pauli matrices

M. V. Berry 1983

♦ Map from $\boldsymbol{k}$ to $\boldsymbol{R}$ as $\boldsymbol{R} = \boldsymbol{R}(\boldsymbol{k})$.

$$\boldsymbol{h}(\boldsymbol{R})|\boldsymbol{R}\rangle_\pm = E_\pm(\boldsymbol{R})|\boldsymbol{R}\rangle_\pm, \qquad E_\pm(\boldsymbol{R}) = \pm R \quad (= \pm|\boldsymbol{R}|)$$

$$|\boldsymbol{R}\rangle = \frac{1}{\sqrt{2R(R-R_z)}} \begin{pmatrix} R_z - R \\ R_x + iR_y \end{pmatrix} = \begin{pmatrix} \sin\frac{\theta}{2} \\ e^{i\phi}\cos\frac{\theta}{2} \end{pmatrix}$$

$|\boldsymbol{R}\rangle = |\boldsymbol{R}\rangle_-$ is the negative energy state and (R, θ, ϕ) is the polar coordinate.

Chern Number and the Covering Number

By the Gauss' Theorem

$$C = -\int_{R(T^2)} dV \; \delta_R(\boldsymbol{R}) = -N_{\text{covering}}$$

$$N_{\text{covering}} = N(R(T), \mathcal{O})$$

How many times the surface $R(T^2)$ wraps around the origin $\mathcal{O}$

$\rightarrow$ New Diffrent but equivalent topological Expression for the Chern number !

$R(T^2)$ for $d_{x^2-y^2} + id_{xy}$ case

$$\boldsymbol{R} = \boldsymbol{R}(\boldsymbol{k}) = (\mathrm{Re}\,\Delta(\boldsymbol{k}), -\mathrm{Im}\,\Delta(\boldsymbol{k}), \epsilon(\boldsymbol{k}))$$

$$\Delta(\boldsymbol{k}) = 2\Delta_{x2-y2}(\cos k_x - \cos k_y) + 2i\Delta_{xy}(\cos(k_x + k_y) - \cos(k_x - k_y))$$

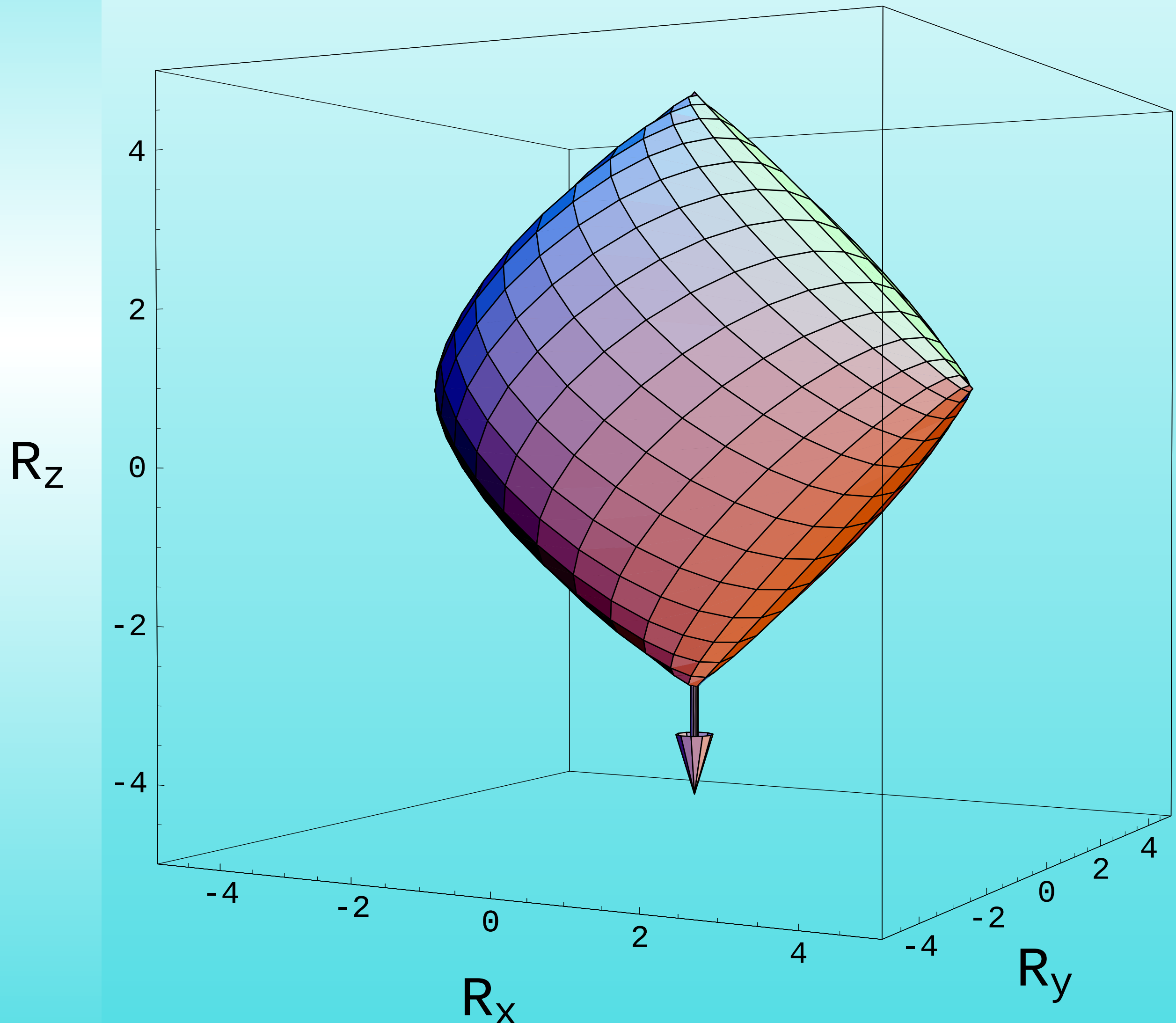

$\Longleftarrow$

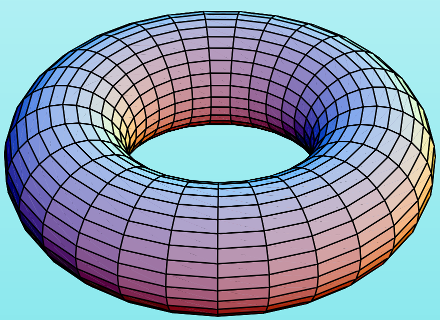

$\Delta_{x2-y2} = t$

$\Delta_{xy} = t$

$\mu = -t,$

$t = 1$

$R(T^2)$ **for** $d_{x^2-y^2} + id_{xy}$ **case**

$$\boldsymbol{R} = \boldsymbol{R}(\boldsymbol{k}) = (\mathrm{Re}\,\Delta(\boldsymbol{k}), -\mathrm{Im}\,\Delta(\boldsymbol{k}), \epsilon(\boldsymbol{k}))$$

$$\Delta(\boldsymbol{k}) = 2\Delta_{x2-y2}(\cos k_x - \cos k_y) + 2i\Delta_{xy}(\cos(k_x+k_y) - \cos(k_x-k_y))$$

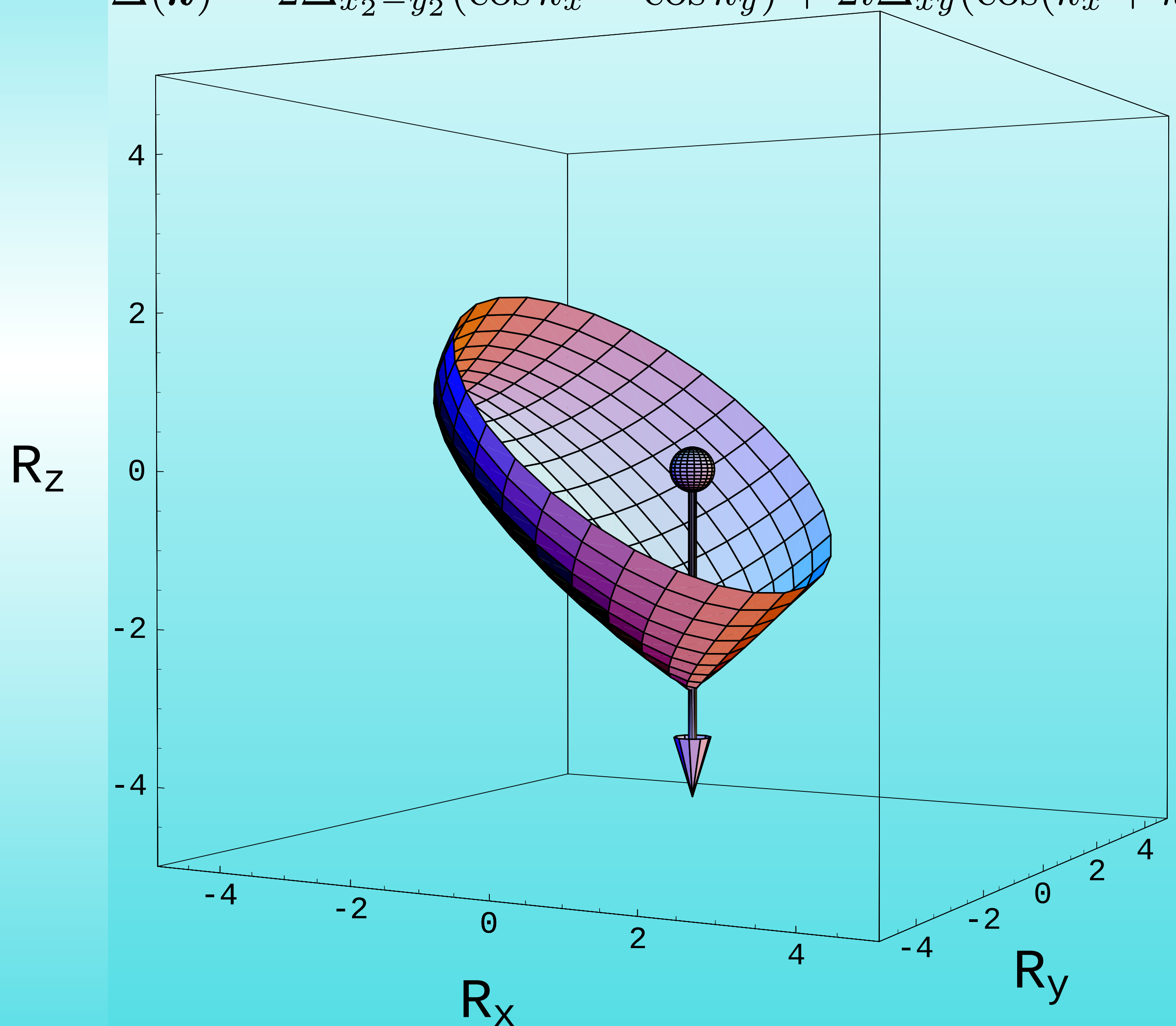

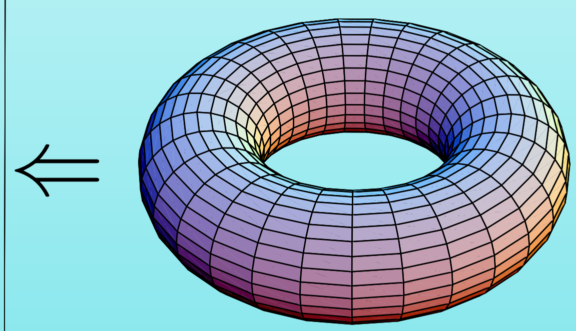

$\Delta_{x2-y2} = t$

$\Delta_{xy} = t$

$\mu = -t,$

$t = 1$

It's doubly covered !

$R(T^2)$ for $d_{x^2-y^2} + id_{xy}$ case

$$\boldsymbol{R} = \boldsymbol{R}(\boldsymbol{k}) = (\mathrm{Re}\,\Delta(\boldsymbol{k}), -\mathrm{Im}\,\Delta(\boldsymbol{k}), \epsilon(\boldsymbol{k}))$$

$$\Delta(\boldsymbol{k}) = 2\Delta_{x2-y2}(\cos k_x - \cos k_y) + 2i\Delta_{xy}(\cos(k_x + k_y) - \cos(k_x - k_y))$$

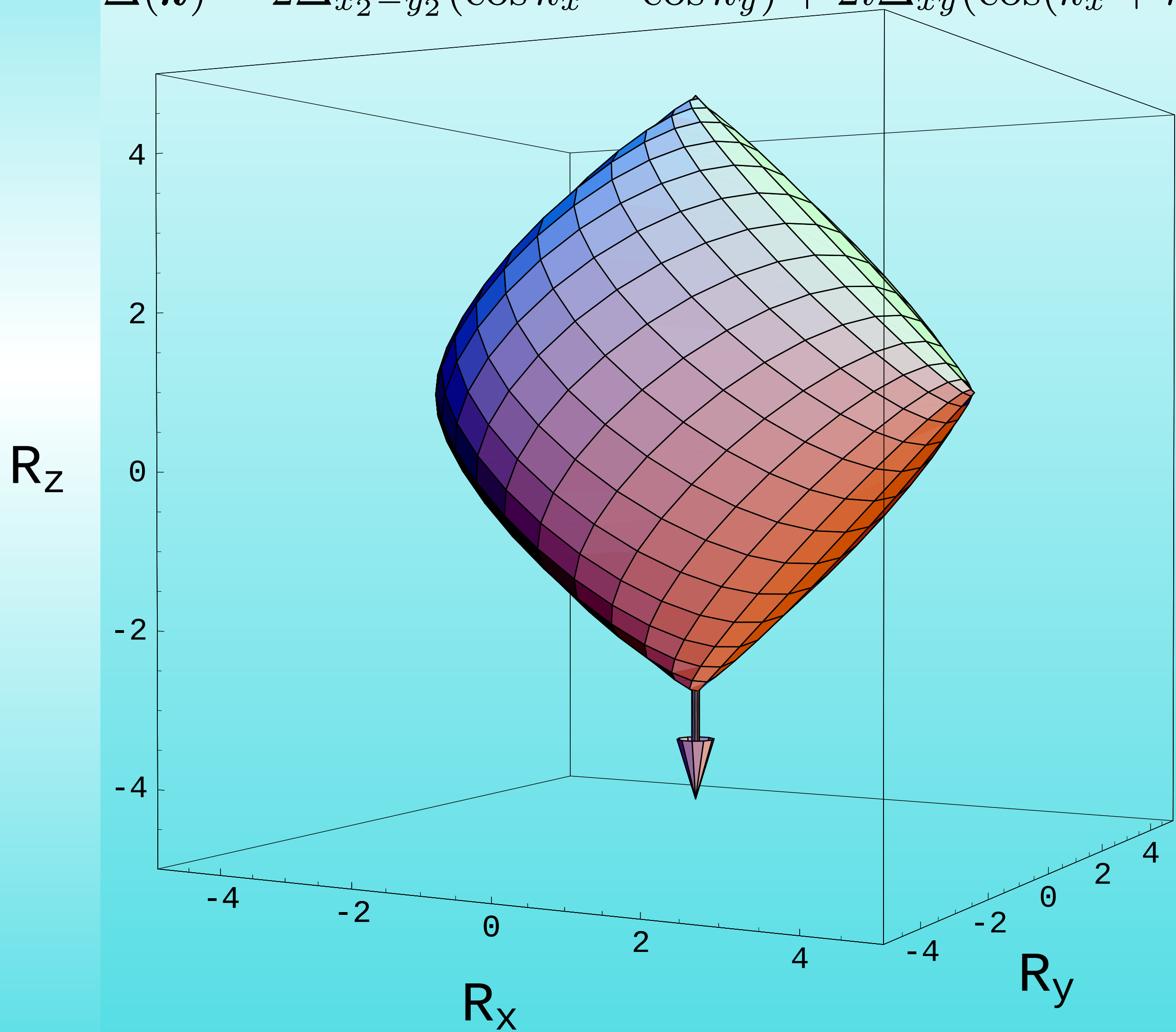

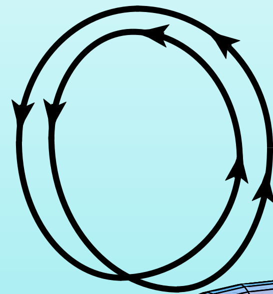

$\Leftarrow$

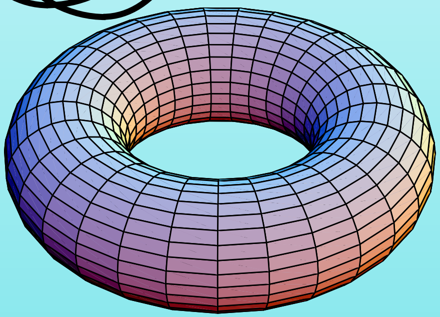

$\Delta_{x2-y2} = t$

$\Delta_{xy} = t$

$\mu = -t,$

$t = 1$

Chiral p case

$$\boldsymbol{R} = \boldsymbol{R}(\boldsymbol{k}) = (\mathrm{Re}\,\Delta(\boldsymbol{k}), -\mathrm{Im}\,\Delta(\boldsymbol{k}), \epsilon(\boldsymbol{k}))$$

$$\Delta(\boldsymbol{k}) = 2i\Delta_x(\sin k_x + i \sin k_y)$$

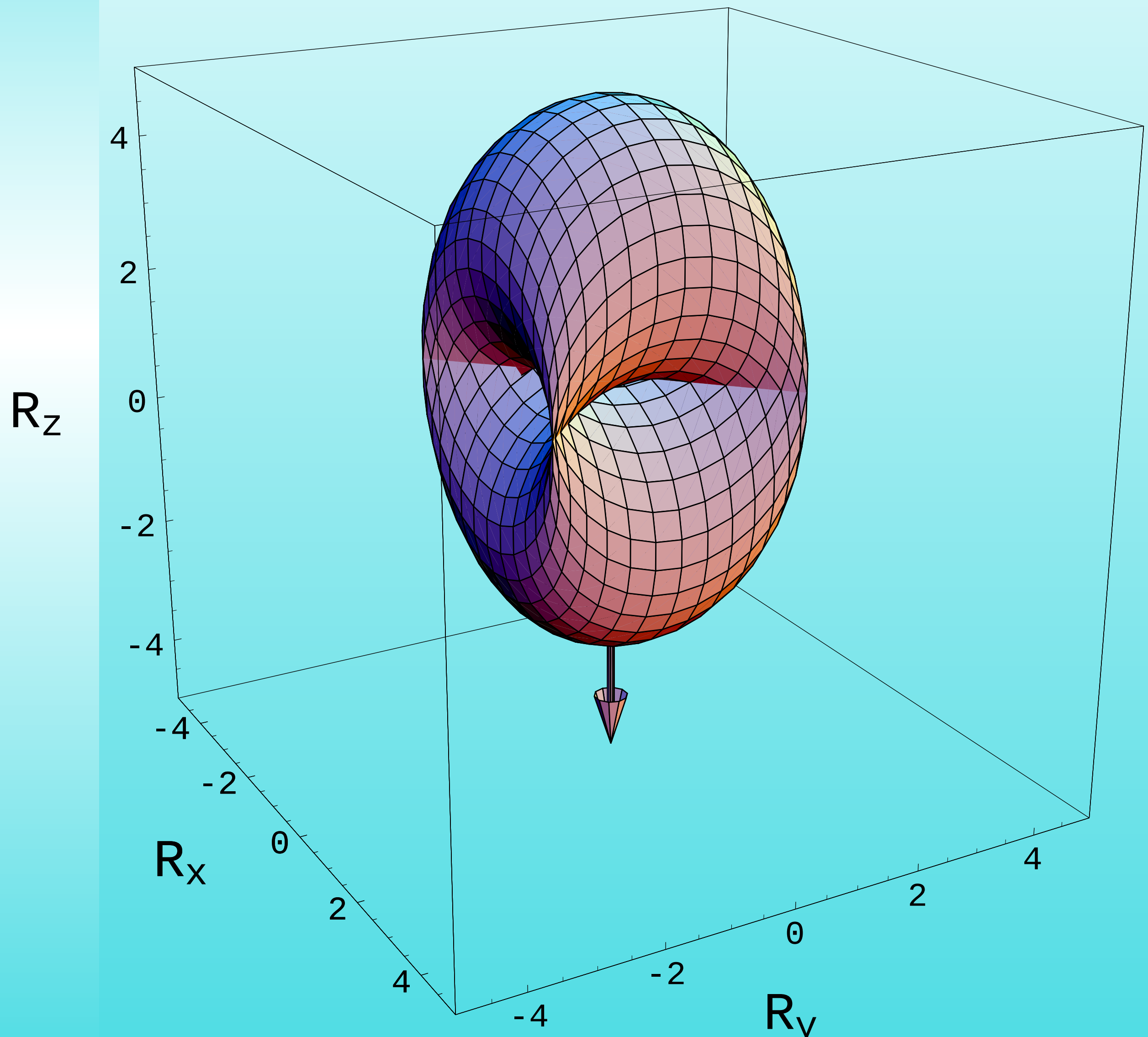

$\Longleftarrow$

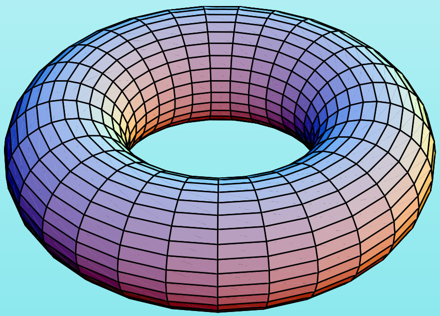

$\Delta_x = -t$

$\mu = -t,$

$t = 1$

Chiral p case

Self-Intersection !
Inside and Outside of the surface Interchange !

$$\boldsymbol{R} = \boldsymbol{R}(\boldsymbol{k}) = (\mathrm{Re}\,\Delta(\boldsymbol{k}), -\mathrm{Im}\,\Delta(\boldsymbol{k}), \epsilon(\boldsymbol{k}))$$

$$\Delta(\boldsymbol{k}) = 2i\Delta_x(\sin k_x + i\sin k_y)$$

Always Orientable

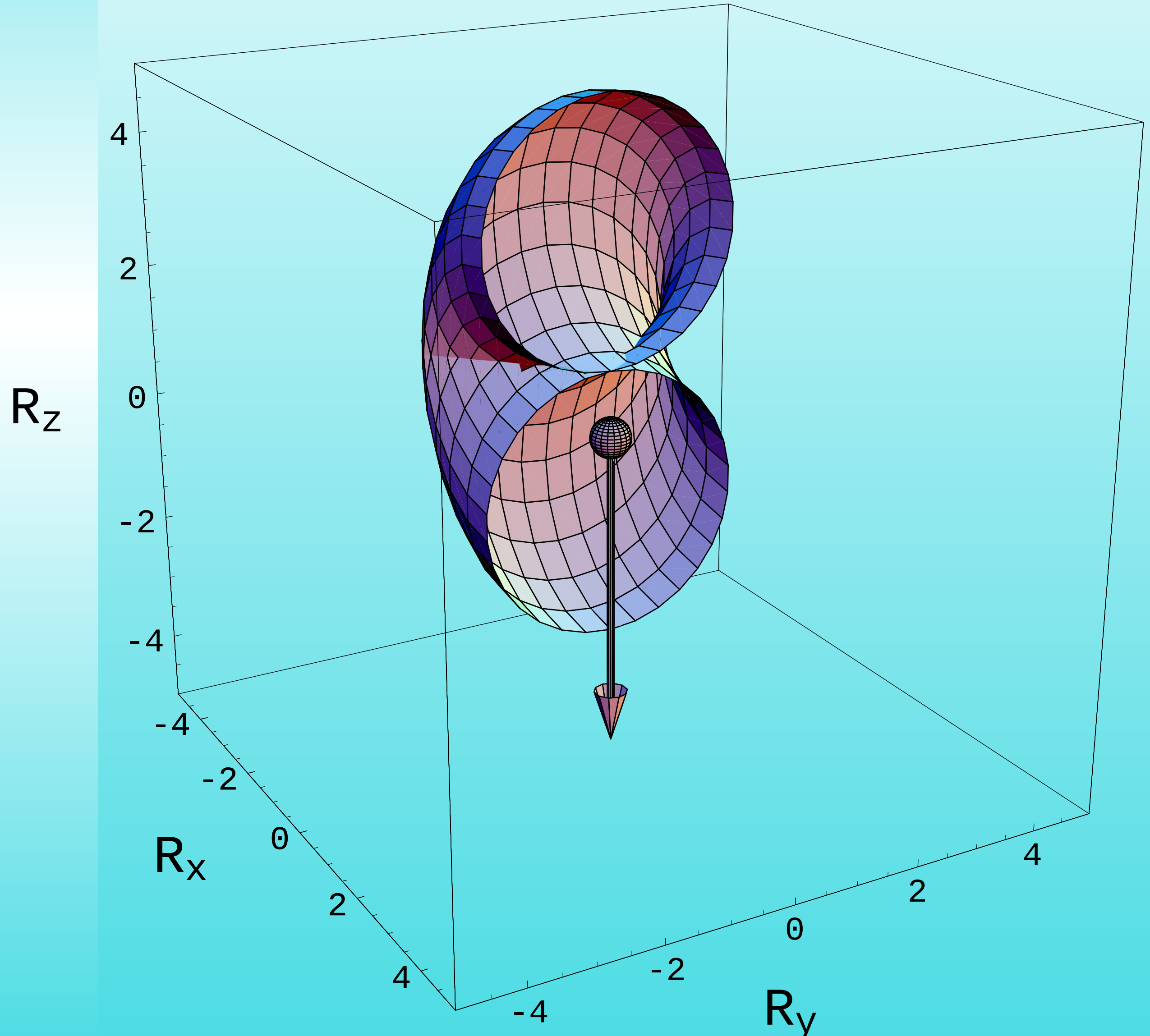

$\Leftarrow$

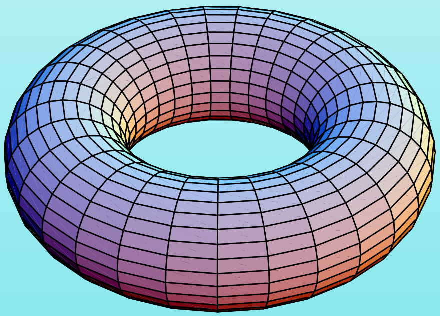

$\Delta_x = -t$

$\mu = -t,$

$t = 1$

Chiral p case

Self-Intersection !
Inside and Outside of the surface Interchange !

$$\boldsymbol{R} = \boldsymbol{R}(\boldsymbol{k}) = (\mathrm{Re}\,\Delta(\boldsymbol{k}), -\mathrm{Im}\,\Delta(\boldsymbol{k}), \epsilon(\boldsymbol{k}))$$

$$\Delta(\boldsymbol{k}) = 2i\Delta_x(\sin k_x + i\sin k_y)$$

Always Orientable

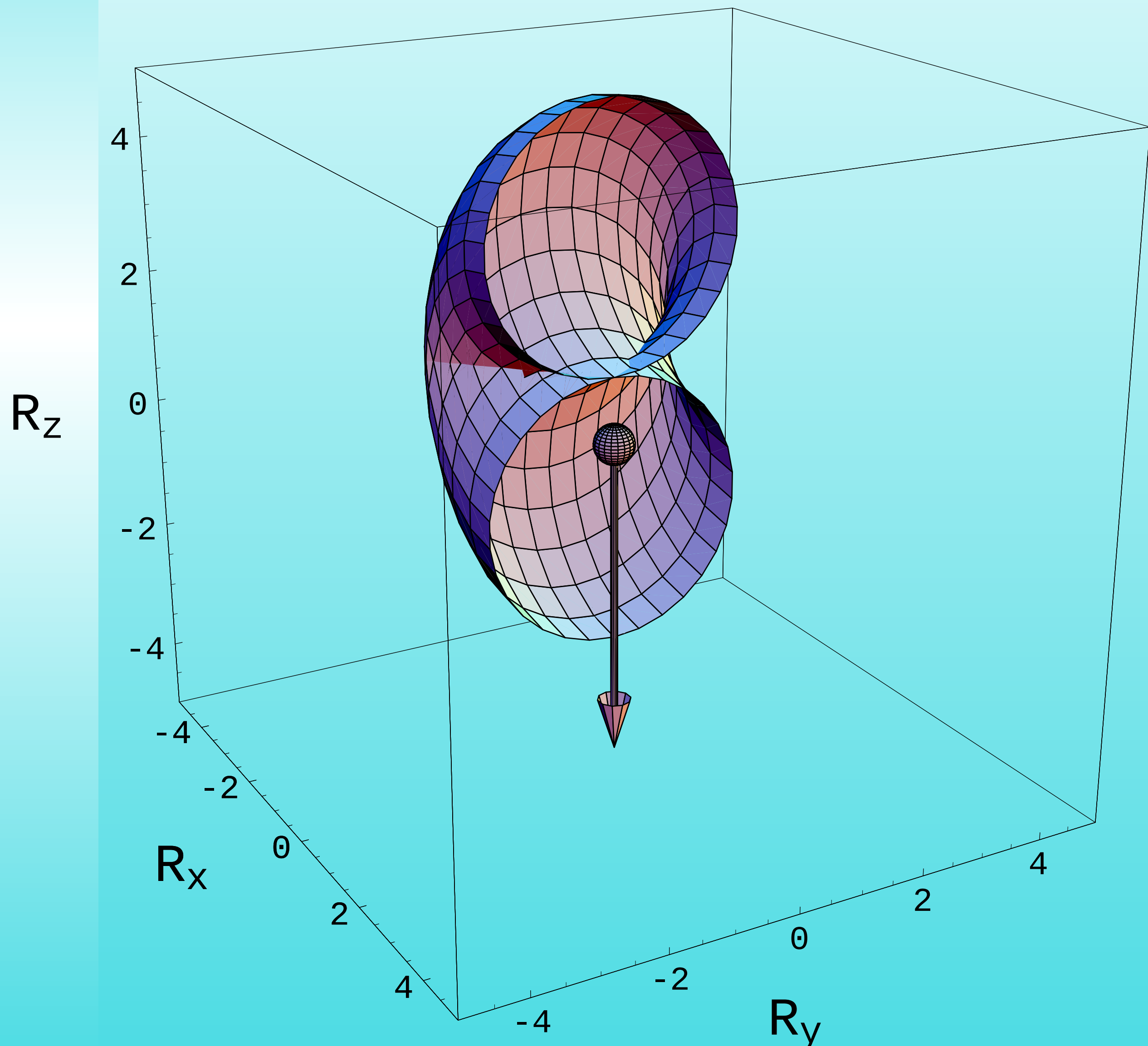

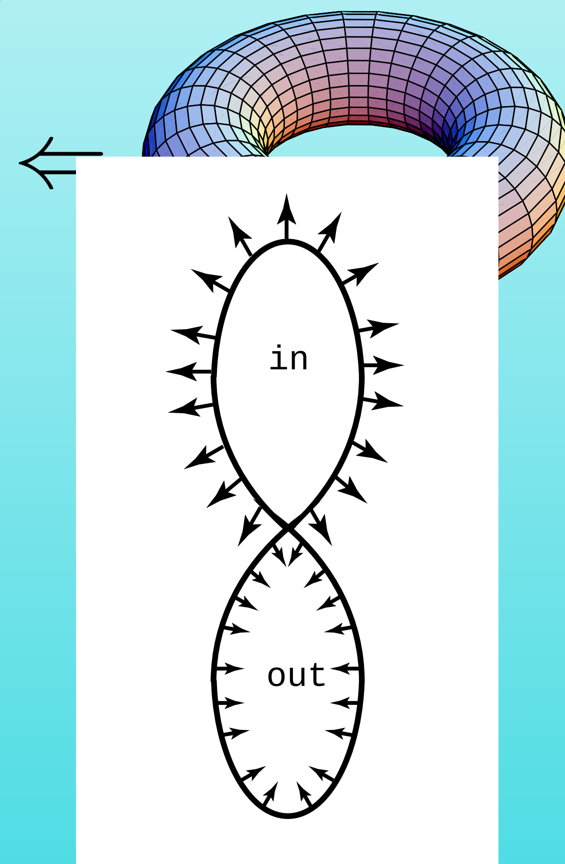

Topological Aspects of (Generic) Superconductors

Generalization for Generic Superconductors

Singlet and Triplet

Unitary order and Nonunitary order

Non-Abelian Gauge Structure

Abelian Chiral Anomaly

(Text Book Example)

Generic BdG Hamiltonian

$$H=\sum_{ij}t_{ij}c^\dagger_{i\sigma}c_{j\sigma}+\sum_{ij}V_{ij}^{\sigma_1\sigma_2;\sigma_3\sigma_4}c^\dagger_{i\sigma_1}c^\dagger_{j\sigma_2}c_{j\sigma_3}c_{i\sigma_4},$$

$$\Rightarrow\mathcal{H}=\sum_{ij}t_{ij}c^\dagger_{i\sigma}c_{j\sigma}+\sum_{ij}(\Delta_{ij}^{\sigma_4\sigma_3*}c_{j\sigma_3}c_{i\sigma_4}+\Delta_{ij}^{\sigma_1\sigma_2}c^\dagger_{i\sigma_1}c^\dagger_{j\sigma_2})$$

$$\Delta_{ij}^{\sigma_1\sigma_2}=V_{ij}^{\sigma_1\sigma_2;\sigma_3\sigma_4}\langle c_{j\sigma_3}c_{i\sigma_4}\rangle=-\Delta_{ji}^{\sigma_2\sigma_1}$$

$$=\sum_k{}'(c^\dagger_{k\uparrow},c^\dagger_{k\downarrow},c_{-k\uparrow}c_{-k\downarrow})\begin{pmatrix}\epsilon_k & 0 & \Delta_k^{\uparrow\uparrow} & \Delta_k^{\uparrow\downarrow}\\ 0 & \epsilon_k & \Delta_k^{\downarrow\uparrow} & \Delta_k^{\downarrow\downarrow}\\ \Delta_k^{\uparrow\uparrow*} & \Delta_k^{\downarrow\uparrow*} & -\epsilon_k & 0\\ \Delta_k^{\uparrow\downarrow*} & \Delta_k^{\downarrow\downarrow*} & 0 & -\epsilon_k\end{pmatrix}\begin{pmatrix}c_{k\uparrow}\\ c_{k\downarrow}\\ c^\dagger_{-k\uparrow}\\ c^\dagger_{-k\downarrow}\end{pmatrix}$$

$$\boldsymbol{h}_k=\begin{pmatrix}\epsilon_k 1_2 & \boldsymbol{\Delta}_k\\ \boldsymbol{\Delta}_k^\dagger & -\epsilon_k 1_2\end{pmatrix},\quad \boldsymbol{\Delta}_{-k}=-\tilde{\boldsymbol{\Delta}}_k$$

$$\boxed{\boldsymbol{\Delta}_k=\begin{cases}\psi_k i\sigma_y & \text{for singlet, } \psi_{-k}=\psi_k,\ \tilde{\boldsymbol{\Delta}}_k=-\boldsymbol{\Delta}_k\\ (\boldsymbol{d}_k\cdot\boldsymbol{\sigma})i\sigma_y & \text{for triplet, } \boldsymbol{d}_{-k}=-\boldsymbol{d}_k,\ \tilde{\boldsymbol{\Delta}}_k=\boldsymbol{\Delta}_k\end{cases}}$$

Particle-Hole Symmetery and Unitarity

$$\boxed{E_k : \begin{pmatrix} \boldsymbol{u}_k \\ \boldsymbol{v}_k \end{pmatrix} \leftrightarrows -E_k : C \begin{pmatrix} \boldsymbol{u}_k \\ \boldsymbol{v}_k \end{pmatrix}}, \quad C = \begin{cases} \rho_x K & \text{for singlet} \\ -i\rho_y K & \text{for triplet} \end{cases}$$

$$(K\varphi = \varphi^*)$$

$$\boxed{\boldsymbol{h}_k^2 = \epsilon_k^2 + \begin{pmatrix} \boldsymbol{\Delta}_k \boldsymbol{\Delta}_k^\dagger & O \\ O & \boldsymbol{\Delta}_k^\dagger \boldsymbol{\Delta}_k \end{pmatrix}}$$

$$\boldsymbol{\Delta}_k \boldsymbol{\Delta}_k^\dagger \propto 1_2 \ ? : \begin{cases} \text{Yes} : \quad \text{Unitary} : \begin{cases} \text{Singlet} \\ \text{Triplet with } \boldsymbol{q}_k = 0 \end{cases} \\ \text{No} : \quad \text{Nonunitary} : \text{Triplet with } \boldsymbol{q}_k \neq 0 \end{cases}$$

$$E_k = \begin{cases} \pm\sqrt{\epsilon_k^2 + |\Delta_k|^2} : (\text{Unitary}) & : \boxed{\boldsymbol{\Delta}_k \boldsymbol{\Delta}_k^\dagger \equiv |\Delta_k|^2 1_2} \\ \pm\sqrt{\epsilon_k^2 + |\boldsymbol{d}_k|^2 \pm q_k} : (\text{Nonunitary}) & : \boxed{\boldsymbol{\Delta}_k \boldsymbol{\Delta}_k^\dagger = |\boldsymbol{d}_k|^2 1_2 + \boldsymbol{\sigma} \cdot \boldsymbol{q}_k} \end{cases}$$

Quasiparticles are doubly degenerated in unitay order!

$$\boxed{\boldsymbol{q}_k = i\boldsymbol{d}_k \times \boldsymbol{d}_k^*} \ (\text{real})$$

$$(\boldsymbol{\sigma} \cdot \boldsymbol{q}_k)\boldsymbol{u}_\pm = \pm q_k \boldsymbol{u}_\pm, \quad q_k = |\boldsymbol{q}_k|$$

Chern Numbers for Unitary states

Degeneracy $\Rightarrow$ Fixing the phases is not enough to define Chern numbers.

Define Non-Abelian Berry's connection (Wilczek-Zee)

$$|\boldsymbol{k}\alpha\rangle = |\alpha\rangle, \quad \alpha = 1, \cdots, M$$

$$A_i^{\alpha\beta} = \langle\alpha|\partial_i|\beta\rangle, \quad \mathcal{A}^{\alpha\beta} = A_i^{\alpha\beta} dk_i, \quad \partial_i = \partial_{k_i}, i = x, y, z$$

$$(\boldsymbol{\mathcal{A}})^{\alpha\beta} \equiv \mathcal{A}^{\alpha\beta},$$

$$\boldsymbol{\mathcal{F}} \equiv d\boldsymbol{\mathcal{A}} + \boldsymbol{\mathcal{A}} \wedge \boldsymbol{\mathcal{A}} = \frac{1}{2!}\boldsymbol{F}_{ij} dk_i \wedge dk_j, \quad \boldsymbol{F}_{ij} = \partial_i \boldsymbol{A}_j - \partial_j \boldsymbol{A}_i + [\boldsymbol{A}_i, \boldsymbol{A}_j]$$

Base change of the degenerate states induces the followings

$$|\alpha\rangle \to |\bar{\alpha}\rangle = |\alpha\rangle \omega^{\alpha\bar{\alpha}}, \quad \boldsymbol{\omega} : \text{unitary}$$

$$\bar{\boldsymbol{\mathcal{A}}} = \boldsymbol{\omega}^\dagger \boldsymbol{\mathcal{A}} \boldsymbol{\omega} + \boldsymbol{\omega}^\dagger d\boldsymbol{\omega}$$

$$\bar{\boldsymbol{\mathcal{F}}} = \boldsymbol{\omega}^\dagger \boldsymbol{\mathcal{F}} \boldsymbol{\omega}$$

$$\mathrm{Tr}\, \bar{\boldsymbol{\mathcal{F}}} = \mathrm{Tr}\, \boldsymbol{\mathcal{F}}$$

$\Leftarrow$ Independent of the bases

Chern Numbers for Unitary states (Cont.)

Further the following quantity is an integer

The first Chern number (Chiral Anomaly)

$$\boxed{C_i(k_i) = \frac{1}{2!}\epsilon_{ijk}\frac{1}{2\pi i}\int_{T^2_{jk}} \mathrm{Tr}\,\boldsymbol{\mathcal{F}}}$$

$$C_x(k_x) = \frac{1}{2\pi i}\int_{T^2_{yz}} dk_y dk_z\; B_x$$

$$C_y(k_y) = \frac{1}{2\pi i}\int_{T^2_{zx}} dk_z dk_x\; B_y$$

$$C_z(k_z) = \frac{1}{2\pi i}\int_{T^2_{xy}} dk_x dk_y\; B_z$$

Integers !

$$B_x = \mathrm{Tr}\,\boldsymbol{F}_{yz}, B_y = \mathrm{Tr}\,\boldsymbol{F}_{zx}, B_z = \mathrm{Tr}\,\boldsymbol{F}_{xy}$$

$T^2_{xy\ (yz,zx)}$: 2D Brillouin zone fixed by $k_{z,(y,x)}$

Dirac Monopoles for Unitary States (Basis)

$\boldsymbol{\Delta}_k = |\Delta_k| \boldsymbol{\Delta}_k^0, \qquad \boldsymbol{\Delta}_k^0$: Unitary

$\Rightarrow$ Eigenvalues are pure phases: $\boldsymbol{\Delta}_k^0 |\alpha\rangle_\sigma = e^{-i\phi_\alpha} |\alpha\rangle_\sigma$, $(\alpha = 1, 2)$

$$\text{BdG equation}\ : \begin{pmatrix} \epsilon_k 1_2 & |\Delta_k| \boldsymbol{\Delta}_k^0 \\ |\Delta_k| (\boldsymbol{\Delta}_k^0)^{-1} & -\epsilon_k 1_2 \end{pmatrix} \begin{pmatrix} \boldsymbol{u} \\ \boldsymbol{v} \end{pmatrix} = E_k \begin{pmatrix} \boldsymbol{u} \\ \boldsymbol{v} \end{pmatrix}$$

$$\Rightarrow \begin{pmatrix} \epsilon_k & |\Delta_k| \\ |\Delta_k| & -\epsilon_k \end{pmatrix}_\rho \otimes 1_2 \begin{pmatrix} \boldsymbol{u} \\ \boldsymbol{\Delta}_k^0 \boldsymbol{v} \end{pmatrix} = E_k \begin{pmatrix} \boldsymbol{u} \\ \boldsymbol{\Delta}_k^0 \boldsymbol{v} \end{pmatrix}$$

$E_k = \pm R_k = \pm \sqrt{\epsilon_k^2 + |\Delta_k|^2}$:doubly degenerate by 1_2

Orthonormal states ($\alpha = 1, 2$) for the negative energy band

$$|\psi_\alpha^-\rangle = \begin{pmatrix} \boldsymbol{u}_- \\ \boldsymbol{v}_- \end{pmatrix}_\alpha = \begin{pmatrix} -\sin\frac{\theta}{2} |\alpha\rangle_\sigma \\ e^{i\phi_\alpha} \cos\frac{\theta}{2} |\alpha\rangle_\sigma \end{pmatrix} = |R_\alpha^-\rangle_\rho \otimes |\alpha\rangle_\sigma$$

with $\epsilon_k = R\cos\theta$, $|\boldsymbol{\Delta}_k| = R\sin\theta$

Dirac Monopoles for Unitary States (Connection)

$$
\begin{aligned}
A_i^{\pm\alpha\beta} =& \langle\psi_\alpha^\pm|\partial_i|\psi_\beta^\pm\rangle = \langle R_\alpha^\pm|\partial_i|R_\beta^\pm\rangle_\rho \langle\alpha|\beta\rangle_\sigma + \langle\alpha|\partial_i|\beta\rangle_\sigma, \\
=& A_i^{\pm\alpha\beta}(\rho)\delta_{\alpha\beta} + A_i^{\alpha\beta}(\sigma), \quad \text{(2 contributions)} \\
(\boldsymbol{A}_i^\pm(\rho))^{\alpha\beta} =& A_i^{\pm\alpha\beta}(\rho) = \langle R_\alpha^\pm|\partial_i|R_\beta^\pm\rangle_\rho \\
(\boldsymbol{A}_i(\sigma))^{\alpha\beta} =& A_i^{\alpha\beta}(\sigma) = \langle\alpha|\partial_i|\beta\rangle_\sigma = (\boldsymbol{U}^\dagger\partial_i\boldsymbol{U})_{\alpha\beta}, \quad \boldsymbol{U} = (|1\rangle_\sigma, |2\rangle_\sigma)
\end{aligned}
$$

$$
B_i^\pm = B_i^\pm(\rho) + B_i(\sigma) = B_i^\pm(\rho)
$$

Contiribution from σ space vanishes due to the "Sum rule" :

$$
B_i(\sigma) = \epsilon_{ijk}\mathrm{Tr}\,\partial_j(\boldsymbol{U}^{-1}\partial_k\boldsymbol{U}) = -\epsilon_{ijk}\mathrm{Tr}\,(\boldsymbol{U}^{-1}\partial_j\boldsymbol{U})(\boldsymbol{U}^{-1}\partial_k\boldsymbol{U}) = 0
$$

Dirac Monopoles for Unitary States

$$
\begin{aligned}
C_z(k_z) =& \frac{1}{2\pi i}\int_{T^2_{xy}} B_z = \frac{1}{2\pi i}\int_{T^2_{xy}} dk_x dk_y \sum_\alpha (\partial_x(\boldsymbol{A}^\pm_y(\rho))^{\alpha\alpha} - \partial_y(\boldsymbol{A}^\pm_x(\rho))^{\alpha\alpha}) \\
=& C_z^{\alpha=1}(k_z) + C_z^{\alpha=2}(k_z) \\
=& N_z^{\alpha=1}(k_z) + N_z^{\alpha=2}(k_z)
\end{aligned}
$$

Sum of Two Covering Degrees around the Dirac Monopole at the Origin

$T^2_{xy} \Rightarrow (R_1(T^2_{xy}), R_2(T^2_{xy}))$
1 to 2 map since $\boldsymbol{\Delta}$ is 2×2.

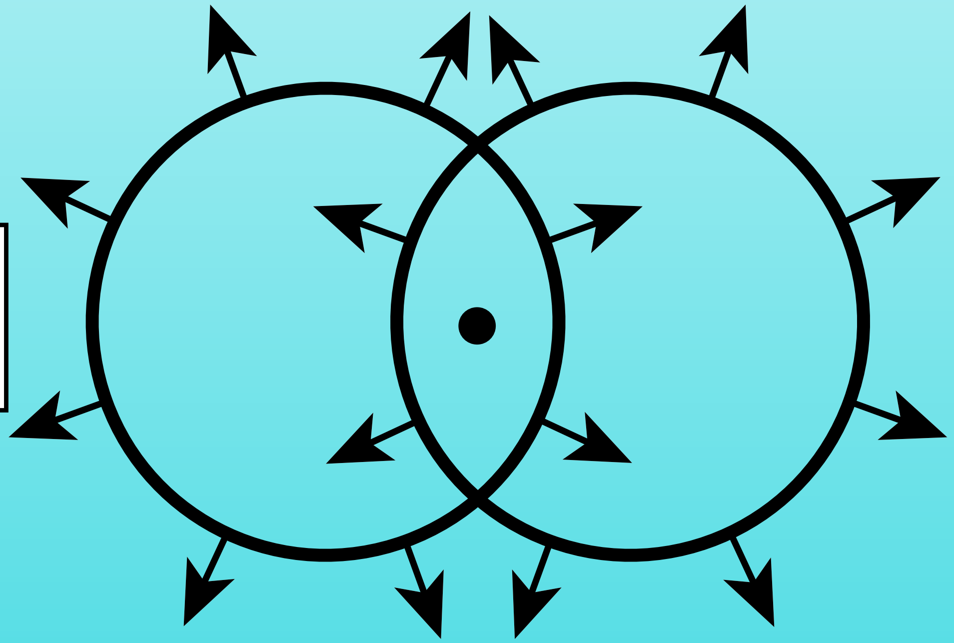

Edge State and Zero Modes

1. Zero Bias Conductance Peak

2. Boundary Magnetism of the Carbon Nanotubes

Zero Energy Edge States in Various Physical Systems

♦ Anisotropic Superconductivity ($d_{x^2-y^2}$-wave)

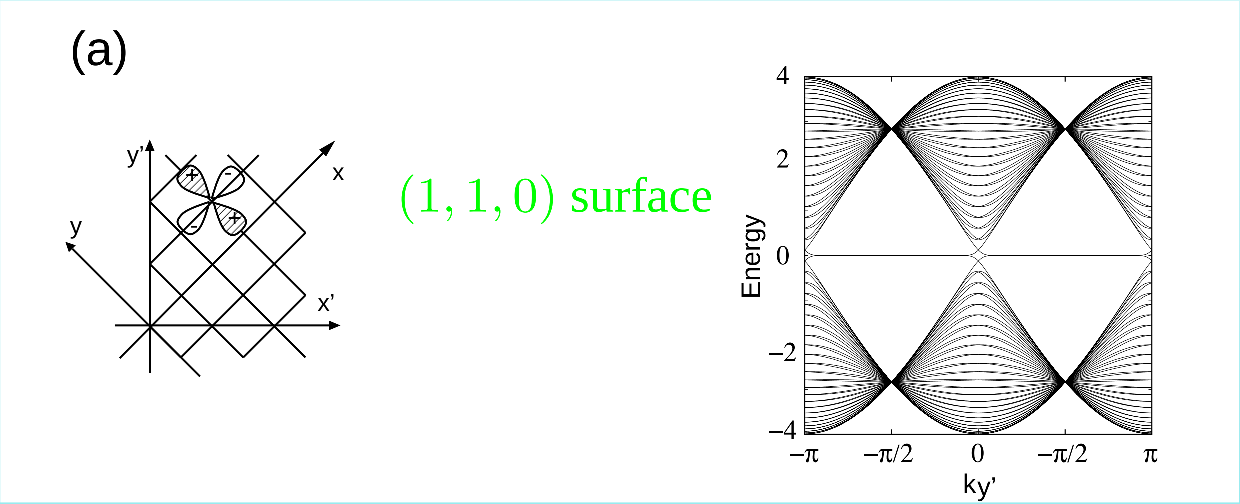

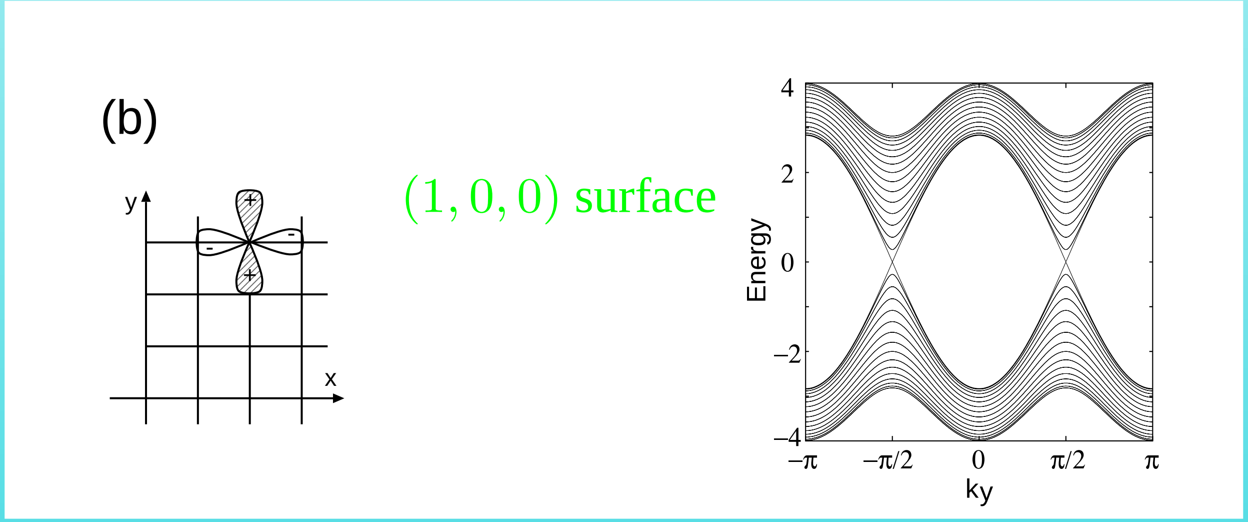

Zero Energy Edge States in Various Physical Systems

- Anisotropic Superconductivity ($d_{x^2-y^2}$-wave)

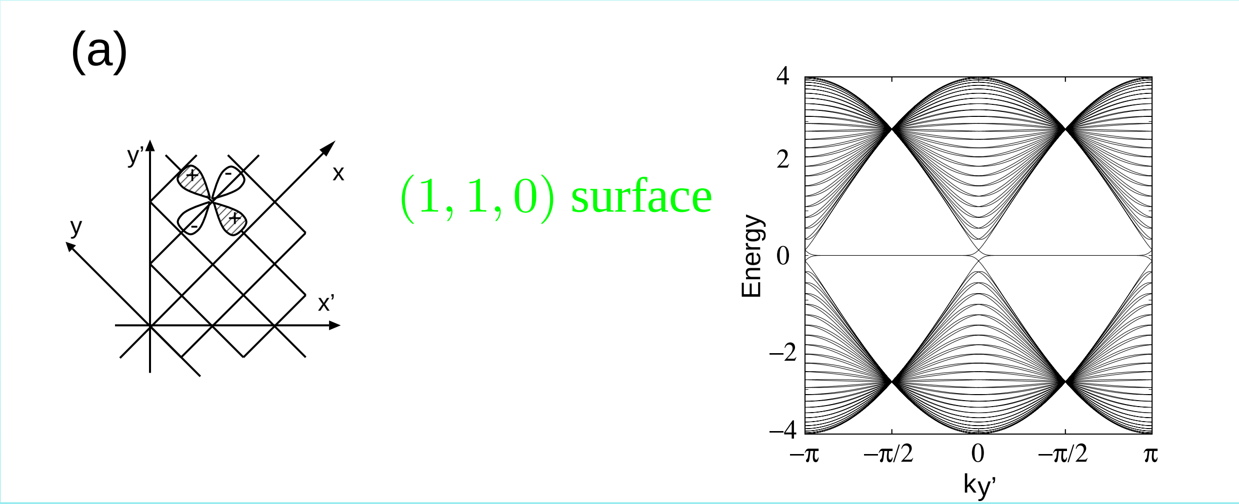

Zero Energy Edge States !

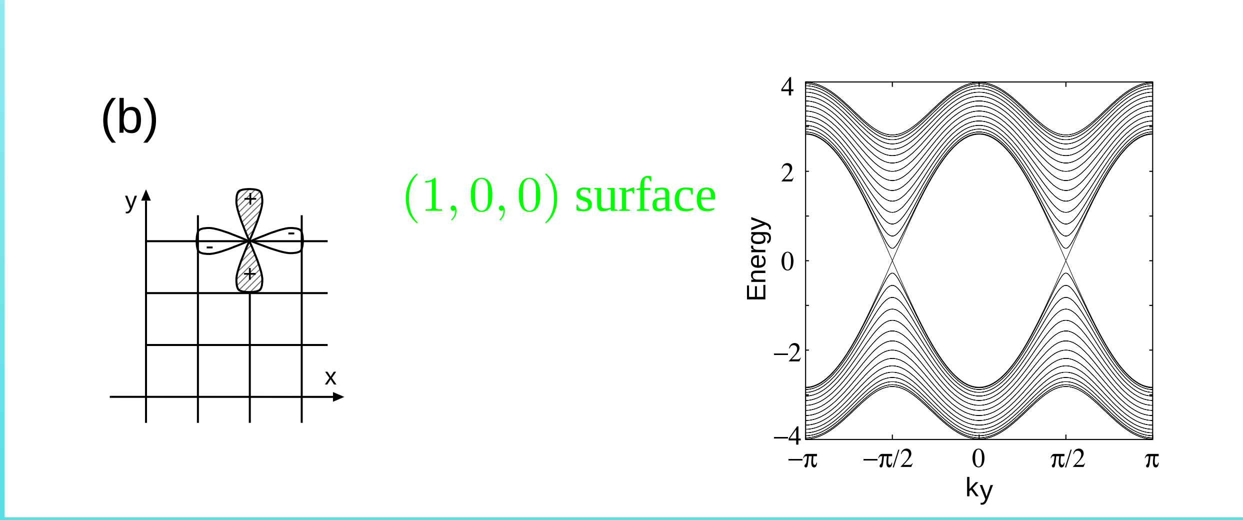

No Edge States !

Zero Energy Edge States : cont.

- Graphite Ribbons (zigzag, bearded, and armchair edges)

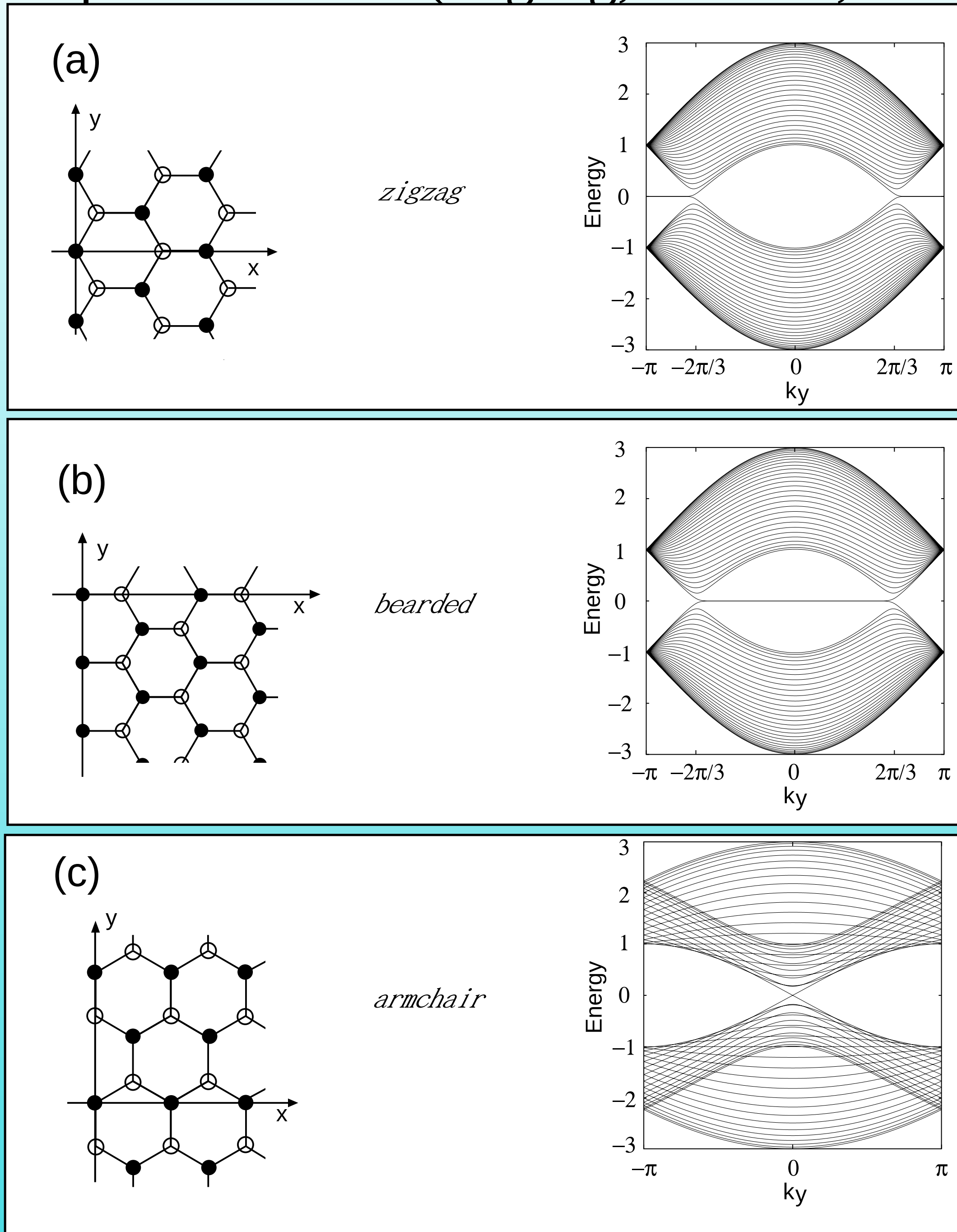

Zero Energy Edge States : cont.

- Graphite Ribbons (zigzag, bearded, and armchair edges)

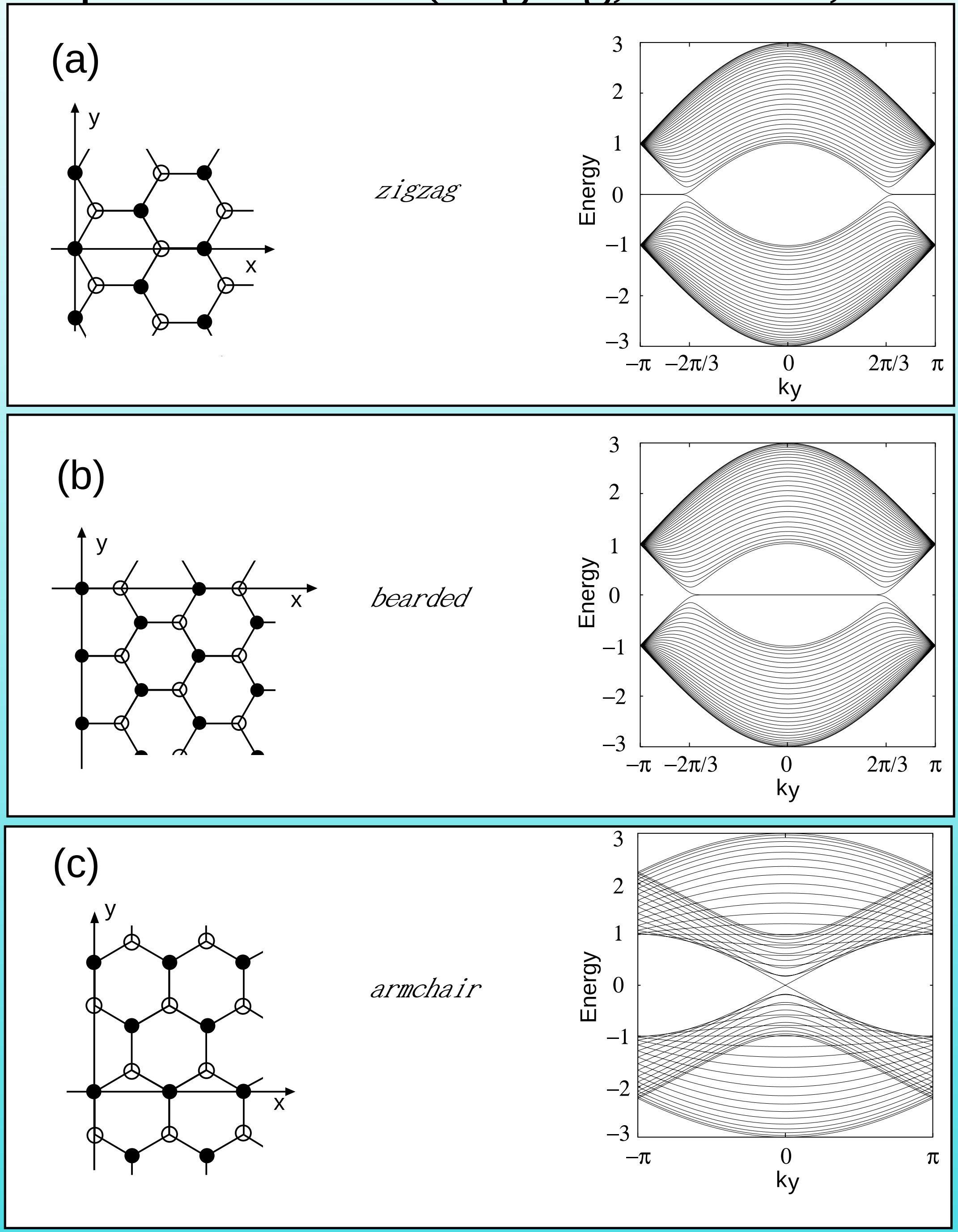

Zero Energy Edge States !

Zero Energy Edge States !

No Edge States !

When and Why the Zero Energy Edge States Appear ?

Accidental ?

No !!

$\Downarrow$

Topological Origin !

- Bulk-Edge Correspondence
- Particle Hole Symmetry
- Topological Stability

S. Ryu and Y. Hatsugai, Phys. Rev. Lett. 89, 077002-1-4 (2002)

Particle Hole Symmetric System

Hamiltonian (in 1D)

$$\mathcal{H} = \sum_{x,x'} \mathbf{c}_x^\dagger h_{x,x'} \mathbf{c}_{x'} \ , \qquad \left(h_{x,x'} = h_{x',x}^\dagger\right)$$

$$\boldsymbol{c}_x = \begin{pmatrix} c_{x\uparrow} \\ c_{x\downarrow} \end{pmatrix} : \text{spinor}, \quad h_{xx'} = \begin{pmatrix} t_{x,x'} & \Delta_{x,x'} \\ \Delta'_{x,x'} & -t_{x,x'} \end{pmatrix}$$

Bulk Hamiltonian (with Translation Symmetry)

$$\mathcal{H}^{bulk} = \sum_k \mathbf{c}_k^\dagger h_k \mathbf{c}_k = \sum_k \mathbf{c}_k^\dagger \begin{pmatrix} \xi_k & \Delta_k \\ \Delta_k^* & -\xi_k \end{pmatrix} \mathbf{c}_k$$

$$E(k) = \pm\sqrt{\xi_k^2 + |\Delta_k|^2}$$

Berry's parametrization

$$h_k = \begin{pmatrix} \xi_k & \Delta_k \\ \Delta_k^* & -\xi_k \end{pmatrix} = \boldsymbol{R}(\boldsymbol{k}) \cdot \boldsymbol{\sigma}$$

$\boldsymbol{\sigma}$: Pauli matrices

$$\boldsymbol{R}(\boldsymbol{k}) = (\mathrm{Re}\,\Delta_k, -\mathrm{Im}\,\Delta_k, \xi_k)$$

- Map from $\boldsymbol{k}$ to $\boldsymbol{R}$ as $\boldsymbol{R} = \boldsymbol{R}(\boldsymbol{k})$.
- In 1D, $k \in S^1$ ($k : 0 \to 2\pi$), so $\boldsymbol{R}$ forms a loop ℓ
  - This map is one to one

A loop in R space characterize the hamiltonian

$$H^{bulk}[\ell]$$

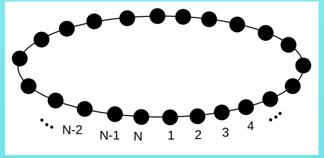

- The system with edges is also constructed by cutting all the matrix elements between the sites 1 and N in real space.

$$H^{edge}[\ell]$$

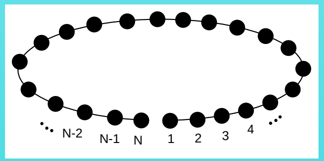

When the Zero Mode Edge States Exist ?

(Sufficient Condition)

I. The loop ℓ is on the plane cutting the origin $\mathcal{O}$.

II. The loop ℓ is continuously deformed to the circle whose

... origin is at $\mathcal{O}$ without passing through $\mathcal{O}$

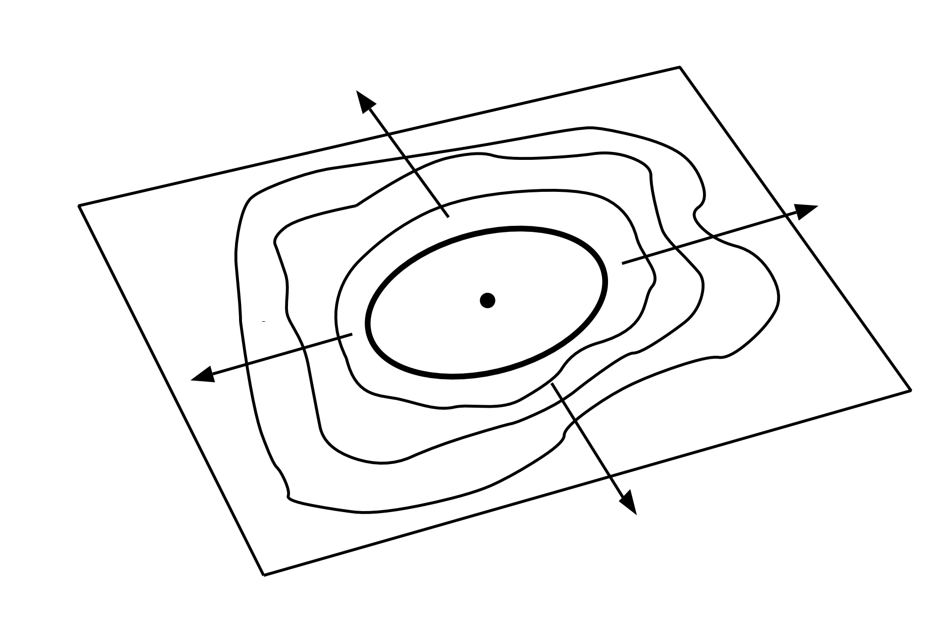

Check for the Anisotropic Superconductivity ($d_{x^2-y^2}$-wave)

♦ (110) surface: the unit cells, loops, and the dispersion

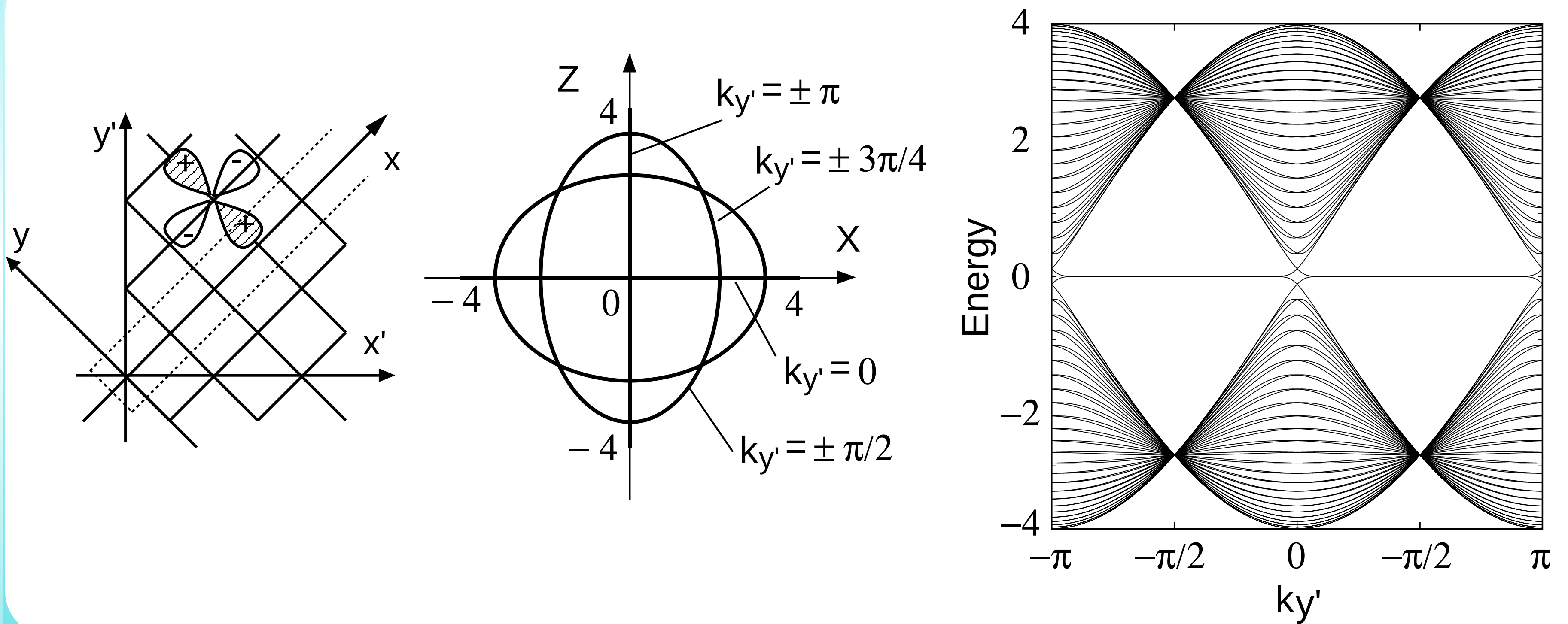

The origin $\mathcal{O}$ is always inside the loop.

Check for the Anisotropic Superconductivity : cont.

- (100) surface: the unit cells, loops, and the dispersion

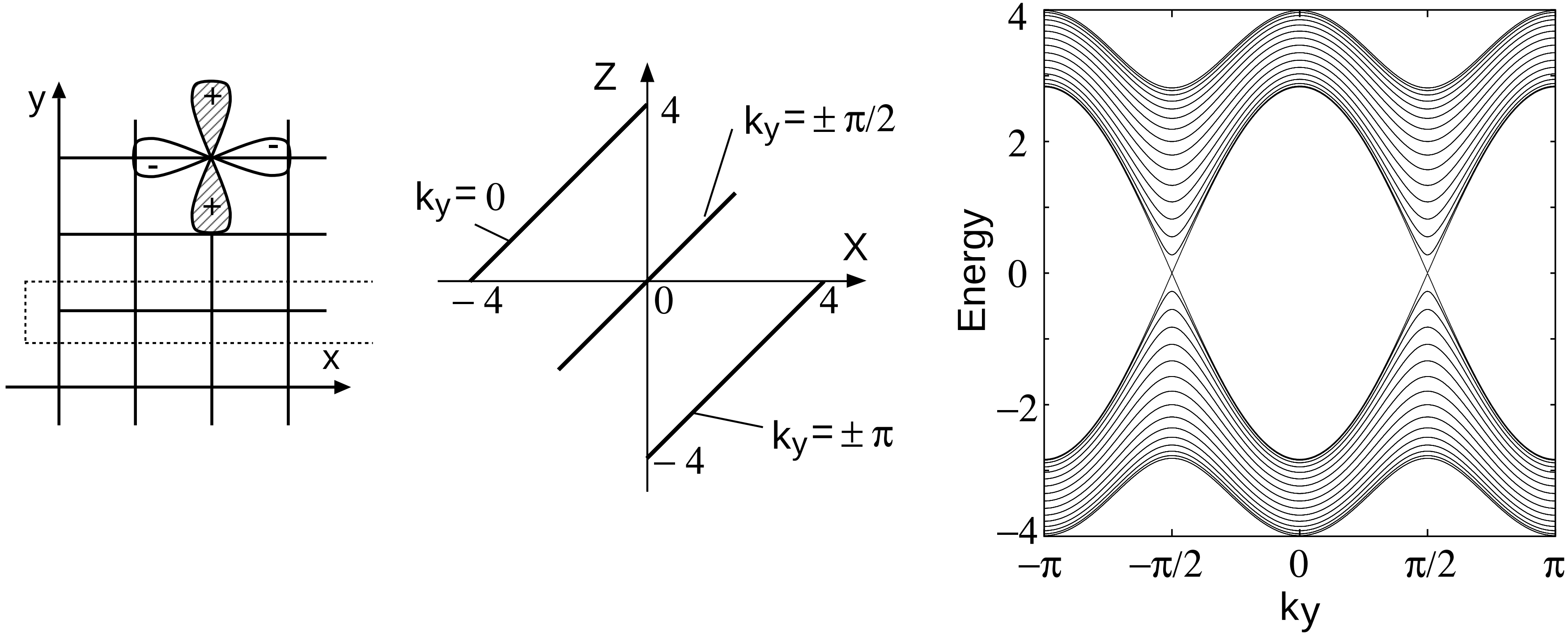

$$\boxed{\text{The origin } \mathcal{O} \text{ is never inside the loop except at } k_y = \pm\pi.}$$

Check for the Graphite Ribbons

♦ Zigzag edge : the unit cells, loops, and the dispersion

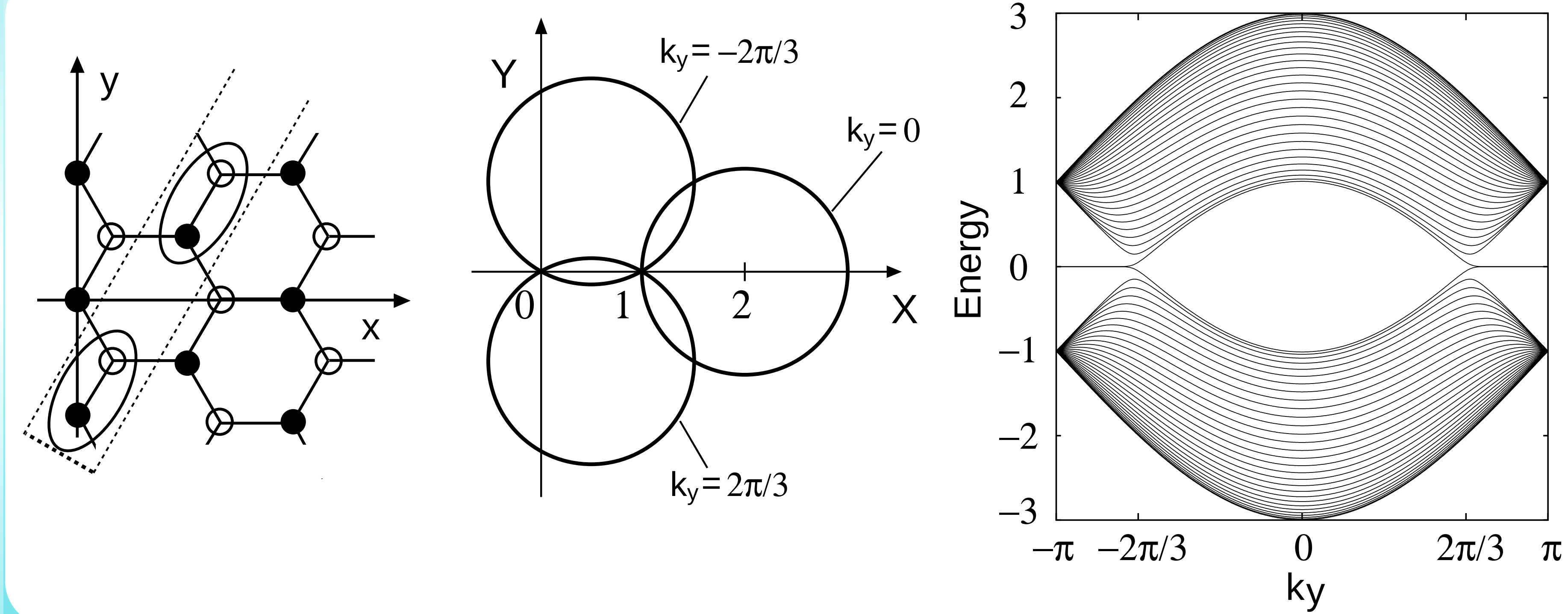

$\boxed{\text{The origin } \mathcal{O} \text{ is inside the loop when } |k_y| > 2\pi/3.}$

Check for the Graphite Ribbons : cont.

♦ Bearded edge : the unit cells, loops, and the dispersion

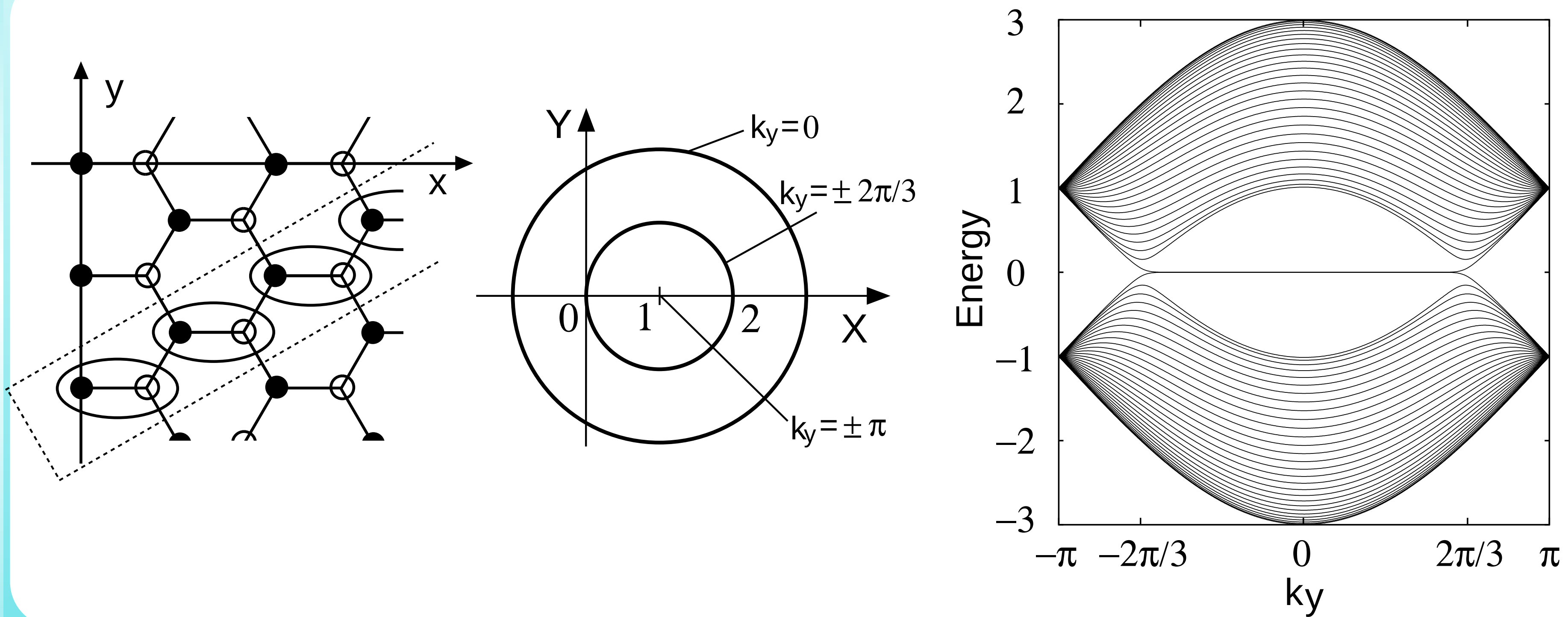

The origin $\mathcal{O}$ is inside the loop when $|k_y| < 2\pi/3$.

Check for the Graphite Ribbons : cont.

♦ Armchair edges : the unit cells, loops, and the dispersion

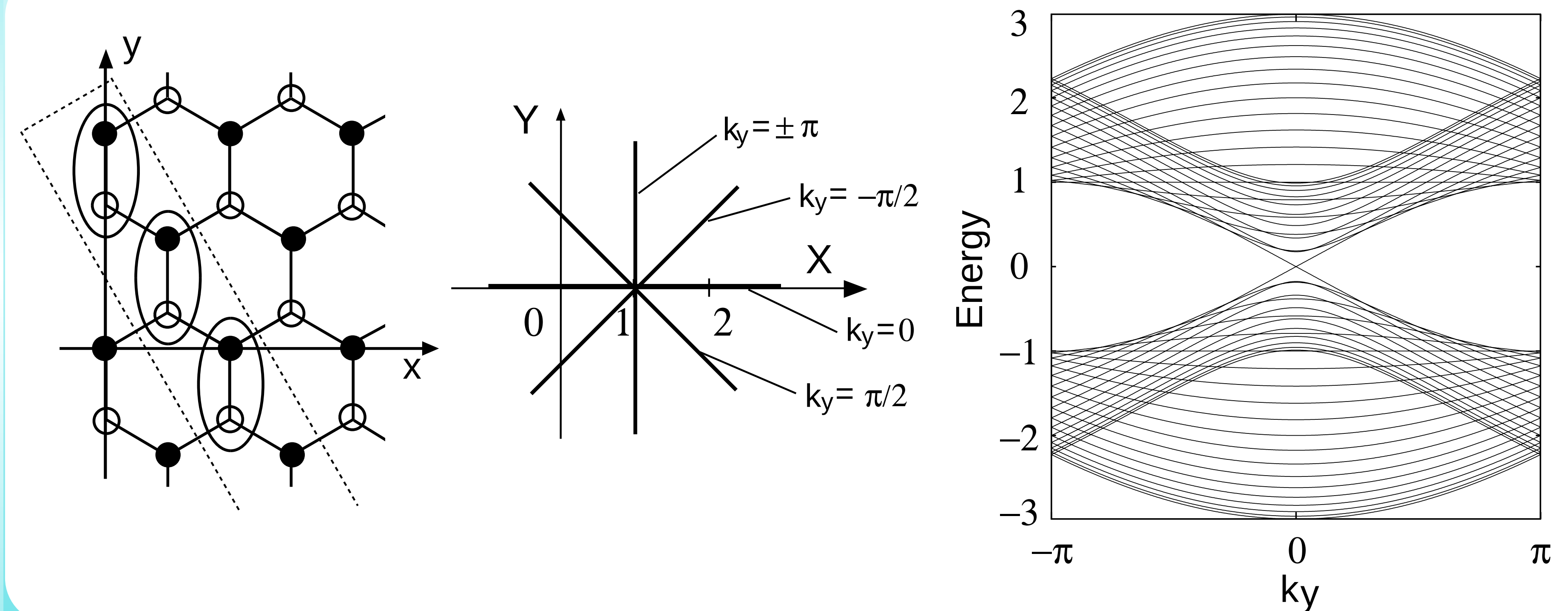

The origin $\mathcal{O}$ is always outside the loop.

Bounary Effects in Anisotropic Superconductivity

- Local (Boundaray) Time Reversal Symmetry Breaking

.   in $d_{x^2-y^2}$-wave Superconductivity

  - As a Peierls Instability of Flat Band Systems

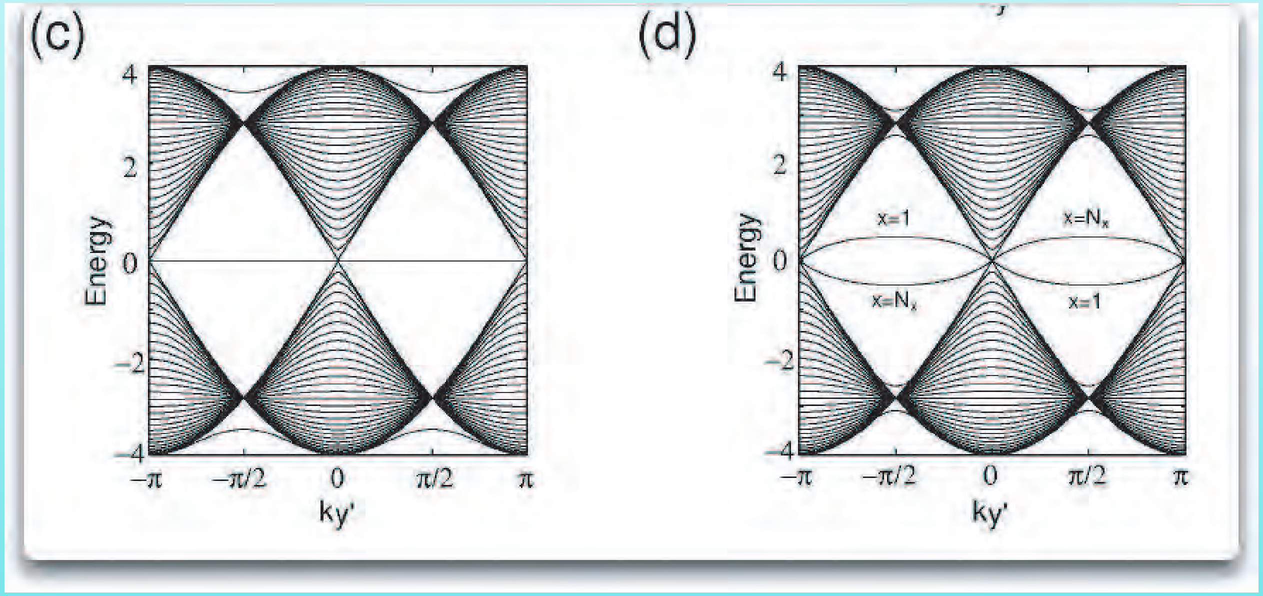

.   with $+s$ with $+is$

S. Ryu and Y.H. to appear in Physica (2003)

Bounary Effects in Carbon Nanotubes

♦ Dimerization Instability by Lattice deformation (Zero mode edge states are protected by the chiral symmetry for a small deformation)

Small dimerization
zero modes

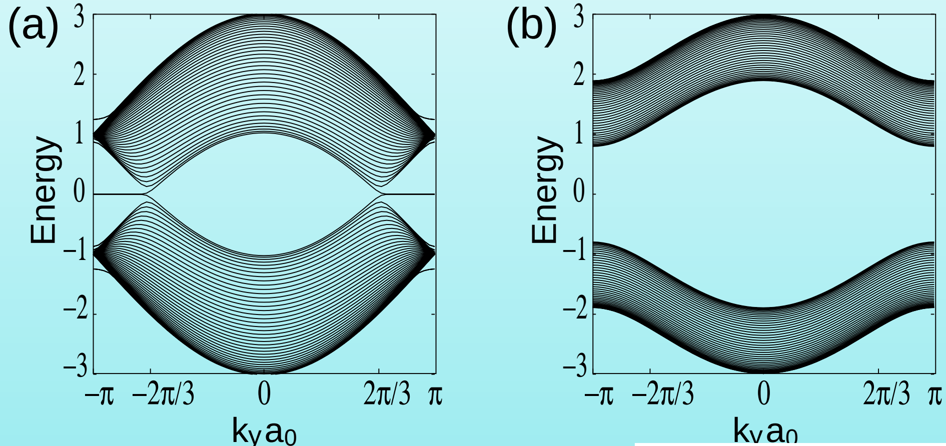

Large deformation
No edge states

Bulk property changed
$\longrightarrow$ no edge states!

♦ Local Spin Moments in the Zig-Zag edges

As a Peierls Instability of Flat Band Systems

Small $U < U_C^{\mathrm{MF}}$
No bulk AF order

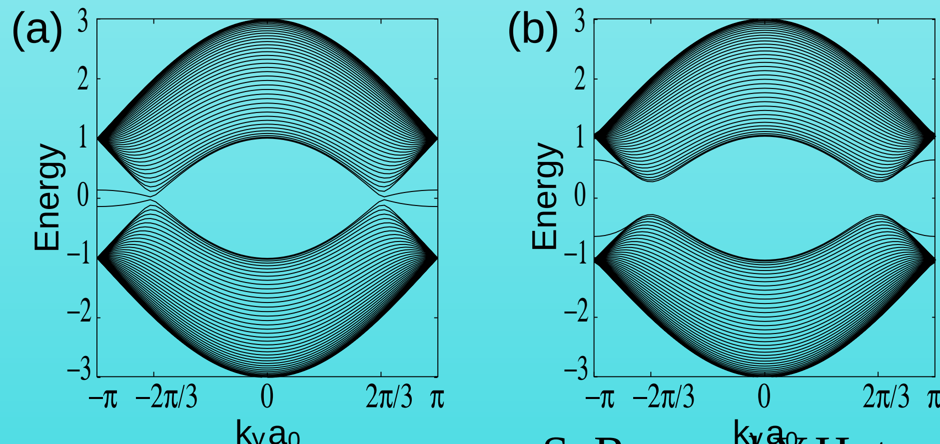

Large $U > U_C^{\mathrm{MF}}$
Bulk is AF ordered

S. Ryu and Y.H. to appear in Physica (2004)

Topological Order

is NOT merely

FANCY

but

USEFUL!